



## Review article



# Lithium-ion batteries for low-temperature applications: Limiting factors and solutions

Ayaulym Belgibayeva<sup>a,b</sup>, Aiyim Rakhmetova<sup>a</sup>, Makpal Rakhmatkyzy<sup>a</sup>, Meruyert Kairova<sup>a</sup>, Ilyas Mukushev<sup>a</sup>, Nurbolat Issatayev<sup>a,b</sup>, Gulnur Kalimuldina<sup>c</sup>, Arailym Nurpeissova<sup>a,b</sup>, Yang-Kook Sun<sup>d,\*\*</sup>, Zhumabay Bakenov<sup>a,b,\*</sup>

<sup>a</sup> Department of Chemical and Materials Engineering, School of Engineering and Digital Sciences, Nazarbayev University, Kabanbay Batyr Ave. 53, Astana, 010000, Kazakhstan

<sup>b</sup> National Laboratory Astana, Nazarbayev University, Kabanbay Batyr Ave. 53, Astana, 010000, Kazakhstan

<sup>c</sup> Department of Mechanical and Aerospace Engineering, School of Engineering and Digital Sciences, Nazarbayev University, Kabanbay Batyr Ave. 53, Astana, 010000, Kazakhstan

<sup>d</sup> Department of Energy Engineering, Hanyang University, Seoul, 04763, Republic of Korea

## HIGHLIGHTS

- Discussion on failure of LIBs' components at low temperatures is provided.
- Practical solutions to overcome the main low-temperature limitations are discussed.
- Main research flaws of LIBs for ultra-low temperatures are pointed out for tackling.

## ABSTRACT

Modern technologies used in the sea, the poles, or aerospace require reliable batteries with outstanding performance at temperatures below zero degrees. However, commercially available lithium-ion batteries (LIBs) show significant performance degradation under low-temperature (LT) conditions. Broadening the application area of LIBs requires an improvement of their LT characteristics. This review examines current challenges for each of the components of LIBs (anode, cathode, and electrolyte) in an LT environment. In addition, it discusses the possible modification methods and practical solutions for better LT performance of the battery. Finally, several research flaws are pointed out for LT LIBs that deserve greater attention, and tackling them might result in LIBs being operable at ultra-low temperatures.

## 1. Introduction

Energy storage devices play an essential role in developing renewable energy sources and electric vehicles as solutions for fossil fuel combustion-caused environmental issues. Owing to their several advantages, such as light weight, high specific capacity, good charge retention, long-life cycling, and low toxicity, lithium-ion batteries (LIBs) have been the energy storage devices of choice for various applications, including portable electronics like mobile phones, laptops, and cameras [1]. Due to the rapid advancements in modern technologies and the possible application in the sea, aerospace, and military, there is a need for a cost-efficient and reliable energy storage system with excellent performance under harsh conditions, including the extreme temperature environment. LIBs can store energy and operate well in the standard

temperature range of 20–60 °C, but performance significantly degrades when the temperature drops below zero [2,3]. The most frost-resistant batteries operate at temperatures as low as –40 °C, but their capacity decreases to about 12% [4]. Furthermore, the aging rate of LIBs accelerates during cycling at low temperatures, thus limiting the long-term use of the battery in cold regions [5].

The primary cause of the low-temperature (LT) degradation has been associated with the change in physical properties of liquid electrolyte and its low freezing point, restricting the movement of Li<sup>+</sup> between electrodes and slowing down the kinetics of the electrochemical reactions [5]. On the other hand, recent studies showed that improving the properties of only electrolytes is insufficient, as changes in properties of electrode materials, including but not limited to the decreased conductivities of electrons and Li<sup>+</sup> because of excessive passivation film

\* Corresponding author. Kabanbay Batyr Ave. 53, Nur-Sultan, 010000, Kazakhstan.

\*\* Corresponding author. Haengdang-dong, Seongdong-gu, Seoul, 133-791, Republic of Korea.

E-mail addresses: [yksun@hanyang.ac.kr](mailto:yksun@hanyang.ac.kr) (Y.-K. Sun), [zbakenov@nu.edu.kz](mailto:zbakenov@nu.edu.kz) (Z. Bakenov).

(cathode-electrolyte interphase (CEI) and anode solid electrolyte interphase (SEI) formation, also significantly contribute to the LT degradation of LIBs [2,3].

Two main approaches have been proposed to overcome the LT limitations of LIBs: coupling the battery with a heating element to avoid exposure of its active components to the low temperature and modifying the inner battery components. Heating the battery externally causes a temperature gradient in the direction of its thickness. Even though the temperature uniformity could be improved by an intermittent heating method, it still requires additional energy, heating devices, and thermal management systems, increasing the mass and volume of the battery system and lowering the energy efficiency [6]. Additionally, modification of components inside the battery does not compromise the gravimetric and volumetric capacities of the battery to the extent that additional heating devices do.

In previous review papers, authors discussed the problems and modifications of electrolyte and electrode materials in general, providing an outlook on the potential LT behavior of most modified battery components with improved room-temperature properties [7–10]. On the other hand, experimental data has been collected on the fundamental LT properties of all battery components with different chemistries since then and reviewed from different numerous perspectives in recent years. Gupta and Manthiram provided a perspective on the LT potential of various advanced chemistries, including lithium-metal, lithium-sulfur, and dual-ion batteries [11]. Other recent reviews explored methods and mechanisms for improving the LT properties of LIBs, emphasizing the electrolyte, cathode materials, anode materials, or lithium metal alone [1,12–18]. For example, Wang et al. discussed various high-energy cathode materials including polyanionic compounds, layered oxides, spinel oxides, Prussian blue and analogs for LT metal-ion batteries [19]. Hou et al. summarized the fundamentals and challenges of LIBs in a wide range of operating temperatures, highlighting the CEI and SEI problems at low temperatures [20]. Piao et al. focused more on heating techniques and thermal management to control the external reaction temperature [21]. The most recent reviews dissected the  $\text{Li}^+$  transport/diffusion in electrolyte, solid electrode and their interphase, temperature-dependent limiting factors and challenges of lithium batteries, and offered their strategies to make an improvement [22–27].

This review provides a comprehensive discussion of the failure mechanisms during the LT operations of all main LIB components (anode, cathode, and electrolyte) and practical solutions to overcome the main LT limitations. Various modern improvement approaches to anode materials are outlined from the LT performance perspective, including modifying commercial anode materials and applying novel ones with enhanced LT capability. Next, different cathode materials and enhancement methods are reviewed, highlighting the promising solutions for mainstream cathodes. Finally, special attention is paid to the approaches used in modifying electrolytes to improve the LT operation of LIBs. Being one of the biggest review papers in the topic, it covers most of the published papers over several decades summarizing them into tables with full information about studied battery configurations and obtained LT performances. It is designed to serve as a guide of available works on the LT LIBs which allows the reader to find new unresearched directions.

## 2. Essential problems affecting the LIB performance at low temperatures

Low ambient temperature causes a significant cell resistance and polarization, leading to a lower state of charge (SOC, defined in %, where 100% means the maximum number of  $\text{Li}^+$  that can be fully reversibly intercalated or de-intercalated in the applied voltage region) of electrodes, and causing a significant decrease of the capacity and faster degradation upon continuous cycling [28,29]. The increased resistance at low temperatures is believed to be mainly associated with

the changed migration behavior of  $\text{Li}^+$  at each battery component, including electrolyte, electrodes, and electrode-electrolyte interphases [21,26]. Being a  $\text{Li}^+$  conducting medium, high-freezing-point electrolyte remains the main rate-limiting factor for different LIB systems at low temperatures. The increased viscosity of the electrolyte at low temperatures decreases the conductivity of  $\text{Li}^+$  in electrolytes and increases the resistance of passivation SEI and CEI layers [30,31].

Later in situ studies on the failure mechanisms of commercial batteries at low temperatures revealed significant negative impacts coming from the side of the electrodes [32,33]. Thus, in the systems with specially-designed low-temperature electrolytes, decreased rate of diffusion of  $\text{Li}^+$  in the solid-state thick electrodes becomes the rate-limiting factor [21]. Moreover, the degradation of electrode materials at low temperatures occurs in both overall electrode levels, including binders, conductive carbons, current collectors, and the atomic level of electrochemically active materials [5,22,34]. Choosing an appropriate binder for both cathode and anode is essential, as the low electrical conductivity of the polymer binder causes additional resistance at low temperatures [35]. Furthermore, weakening of the binding properties and detachment of the active material from the current collector was observed at a shallow storage temperature of  $-133\text{ }^\circ\text{C}$  [34]. Even though most applications do not require tolerance for such extreme conditions, active electrode materials, especially anodes, are more sensitive to temperature changes at the atomic level.

The main limitations of both electrode materials at low temperatures are significant polarization, slow charge transfer kinetics, and high resistance, caused by decreased conductivity of electrons and  $\text{Li}^+$  and the formation of unstable or too thick insulating SEI or CEI layers. When low-freezing-point electrolytes are used and electrodes thicknesses are reduced, desolvation of  $\text{Li}^+$  and its migration through insulating layers to electrodes become the most critical step [21]. On the other hand, studies showed that the anode part of LIBs at low operating temperatures contributes more to the overall cell resistance than the cathode part [32]. Moreover, deposition of metallic lithium and growth of dendrites, formed from the side reactions with electrolyte during charging, shorten battery life and cause safety problems [36,37]. The LT effect on the cathode is studied more diminitively than the anode, assuming it inhibits performance mainly due to the interconnected processes [3]. Depending on the type of batteries and conditions, additional challenges may arise, such as dissolution and deposition of transition metals on the separator, clogging the pores devoted for  $\text{Li}^+$  [33]. Therefore, the physicochemical properties of the separator also play a vital role in sustaining the LT performance of LIBs.

Fig. 1 illustrates the main possible LT limitations of LIBs.

## 3. Anodes

### 3.1. Challenges in anodes at low temperatures

#### 3.1.1. Graphite

Carbon-based materials are often used as the anodes in LIBs, holding the following advantages: low cost, high electrical conductivity, non-toxicity, and stable cycling life [38]. Graphite is the first and the most widely used anode in commercial LIBs because of its charge/discharge profiles, resembling the lithium metal, and the safety of the material at room temperature [39]. However, after careful characterizations of different battery components at low temperatures, it has been found that graphite anode significantly influences the degradation of battery performance at low operating temperatures (Fig. 2a) [2,3,40]. The main challenges include decreased electrical conductivity, restricted diffusion of  $\text{Li}^+$ , and formation of unstable or too thick SEI layer with low conductivity [38,41,42]. High conductivities of electrons and  $\text{Li}^+$  are essential for reversible lithiation of the active anode material. Temperature-dependent lowering of the conductivities leads to increased  $R_{ct}$ , electrode polarization, and poor intercalation/de-intercalation of  $\text{Li}^+$  [43]. It has also been associated

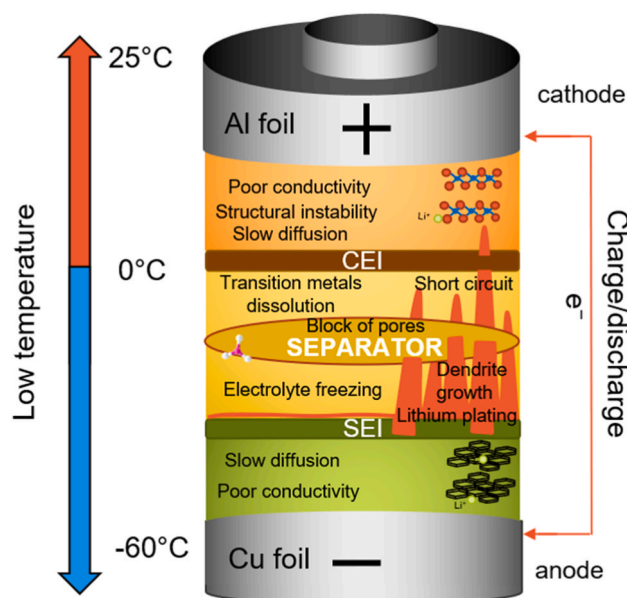


Fig. 1. Illustration of the essential problems affecting the LIB performance at low temperatures.

with the instability of the lithiation products and deposition of the metallic lithium [3].

The formation of a uniform and stable SEI layer of high ionic conductivity on the surface of the anode is also vital for the smooth reversible diffusion of  $\text{Li}^+$  and the cycling efficiency [31,44]. The stability and uniformity of the SEI become a challenge, especially at low operating temperatures below  $0^\circ\text{C}$ . It leads to localized lithium plating and dendrite growth, which can penetrate through the separator to the cathode side, causing short circuit and safety problems [2,3]. Even though some structural modifications can stabilize the SEI layer, irreversible  $\text{Li}^+$  consumption on the surface with the thickening of the SEI layer also limits the diffusion of  $\text{Li}^+$  to the active anode material and, because of its low conductivity, mainly contributes to the increased overall cell resistance [45,46].

Compared to natural graphite, characteristics of synthetic graphite like highly oriented pyrolytic and highly porous graphite, can benefit in the electrochemical properties at LT due to its structural features, like the presence of oxygen groups on the surface of material leading to the more stable SEI layer formation [49]. Park et al. checked five types of graphite including one natural and four synthetic graphite samples, and confirmed that LT properties highly depend on the graphitization degree, surface area, and particle shape of the anode that are easily controlled in synthetic graphites [38]. Thus, all synthetic graphite samples exhibited higher reversible capacities at low temperatures compared to natural one.

### 3.1.2. Silicon (Si)

Si is attracting much interest as one of the most promising materials of anode for applications in LIBs due to its extremely high theoretical capacity ( $3580\text{ mAh g}^{-1}$ ) [50]. Compared to commercially available

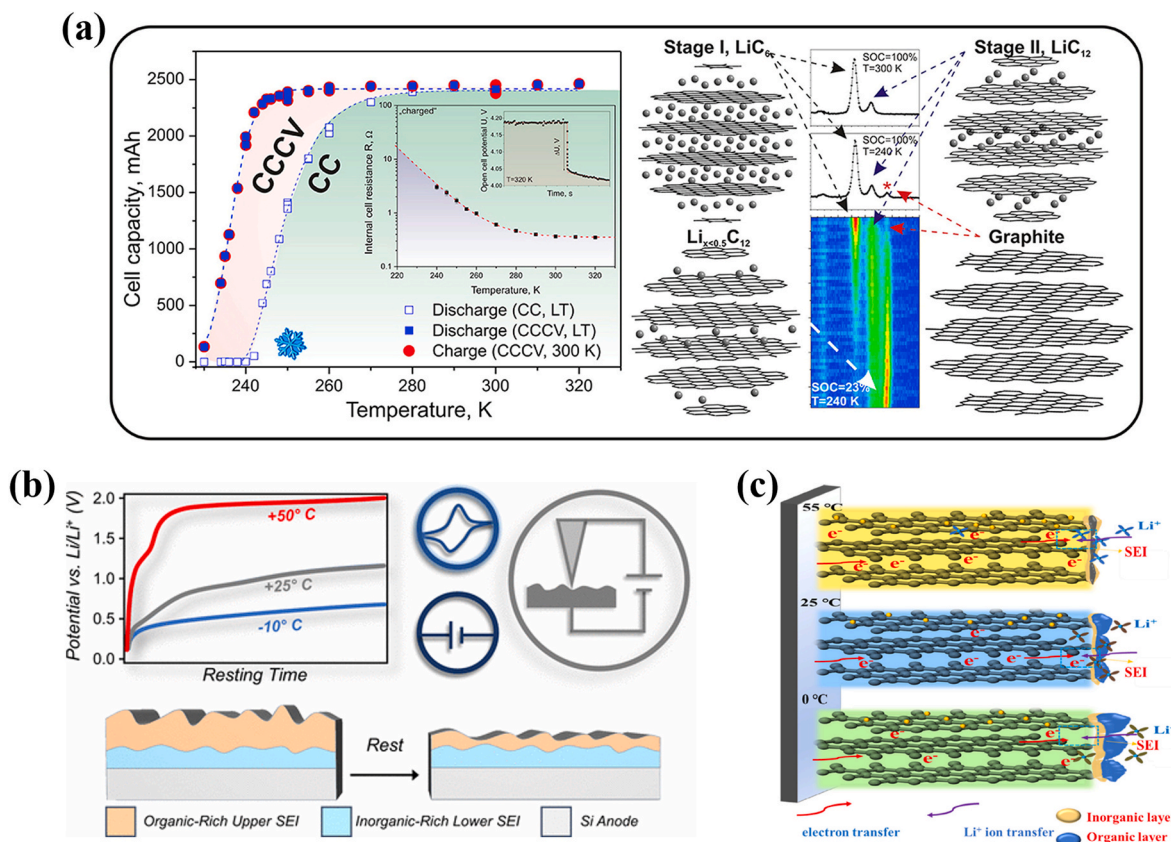


Fig. 2. (a) Effect of low temperature on battery performance and lithiation mechanism of graphite anode. (Reproduced with permission from Ref. [3]. Copyright 2015, Elsevier). (b) Effect of low temperature on the potential of Si anode vs.  $\text{Li}/\text{Li}^+$  and schematics of the SEI features of the Si anode. (Reproduced with permission from Ref. [47]. Copyright 2019, American Chemical Society). Mechanism of the SEI film formation on Si@Graphite@C anodes at different temperatures. (Reproduced with permission from Ref. [48]. Copyright 2022, Elsevier).



carbonaceous materials, Si forms an alloy with lithium, providing higher power density and better  $\text{Li}^+$  diffusivity [51]. However, the disadvantage of such material is rapid collapse upon cycling because of their weak mechanical properties and the volume changes (up to 300%), leading to instability of the SEI layer at a wide range of temperatures [52].

The composition of the SEI layer on Si/electrolyte interphase differs from that of graphite. According to Stetson et al., it consists of two main layers: the low-resistance inorganic-rich side facing the anode and passivating organic-rich side facing the electrolyte [47]. The passivating layer has high solubility at prolonged high-temperature rest but low solubility at low temperatures. Furthermore, the organic-rich SEI layer, in conjunction with the dropped potential of the Si anode vs.  $\text{Li}/\text{Li}^+$  at low temperature (Fig. 2b), potentially causes the lithium plating during LT operations [53].

The incorporation of the graphite into the Si anode can improve the mechanical, chemical, and electrochemical properties of the electrode, giving a synergetic effect from the high theoretical capacity of Si and ultrahigh stability of graphite [54]. On the other hand, the combination of the LT challenges of these two materials occurs unavoidably, leading to poor efficiency during the LT operations (Fig. 2c) [48]. Comprehensive approaches to electrode and electrolyte levels are needed to improve the LT performance of Si/graphite composites.

### 3.2. Approaches to improve the performance of anodes at low temperatures

Anode modifications. Different approaches on the electrode level have been recently proposed to improve the LT properties of the anode part by addressing the main LT limitations mentioned above. As

summarized in Fig. 3, these approaches include controlling the morphology and microstructure, doping and coating nonmetals, metals, and metal ions, modifications on the electrode composition, and finally, coupling carbon-based anode materials with alternative anode materials of higher theoretical capacities and better LT capability than graphite. Table 1 summarizes the reported anode materials with corresponding modifications and LT properties.

#### 3.2.1. Choosing alternative materials

Alternative anode materials for LT applications are proposed based on their working potentials, capacities, electrical and ionic conductivities, stability, and reversibility of electrochemical reactions at low operating temperatures.

Compared to graphite anode, titanium oxides, namely  $\text{Li}_4\text{Ti}_5\text{O}_{12}$  (LTO) and different polymorphs of  $\text{TiO}_2$  (anatase, rutile, brookite, and bronze), have a high operation potential ( $\sim 1.5\text{--}1.7$  V vs.  $\text{Li}/\text{Li}^+$ ) and more stable structure, which allows ensuring higher safety by avoiding plating of metallic lithium at shallow potentials ( $<0.1$  V vs.  $\text{Li}/\text{Li}^+$ ) caused by increased overpotential at low temperatures [63,64,83]. Furthermore, the nature and properties of the SEI layer formed on the surface of these materials are different from that of low-potential anode materials. On the other hand, LTO and  $\text{TiO}_2$  suffer from poor electrical and lithium ionic conductivity, becoming even more severe at low temperatures. Designing binder-free electrode consisting of LTO composite with highly-conductive agents, such as carbon nanotubes (CNT) and Ag nanocrystals, were proposed as a possible solution [62].

Alloying materials, including group IVA elements (Sn, Ge), are extensively studied as alternatives to Si and graphite, but they suffer from colossal volume expansion and structural instability. One way to improve the structural stability and LT performance of alloying

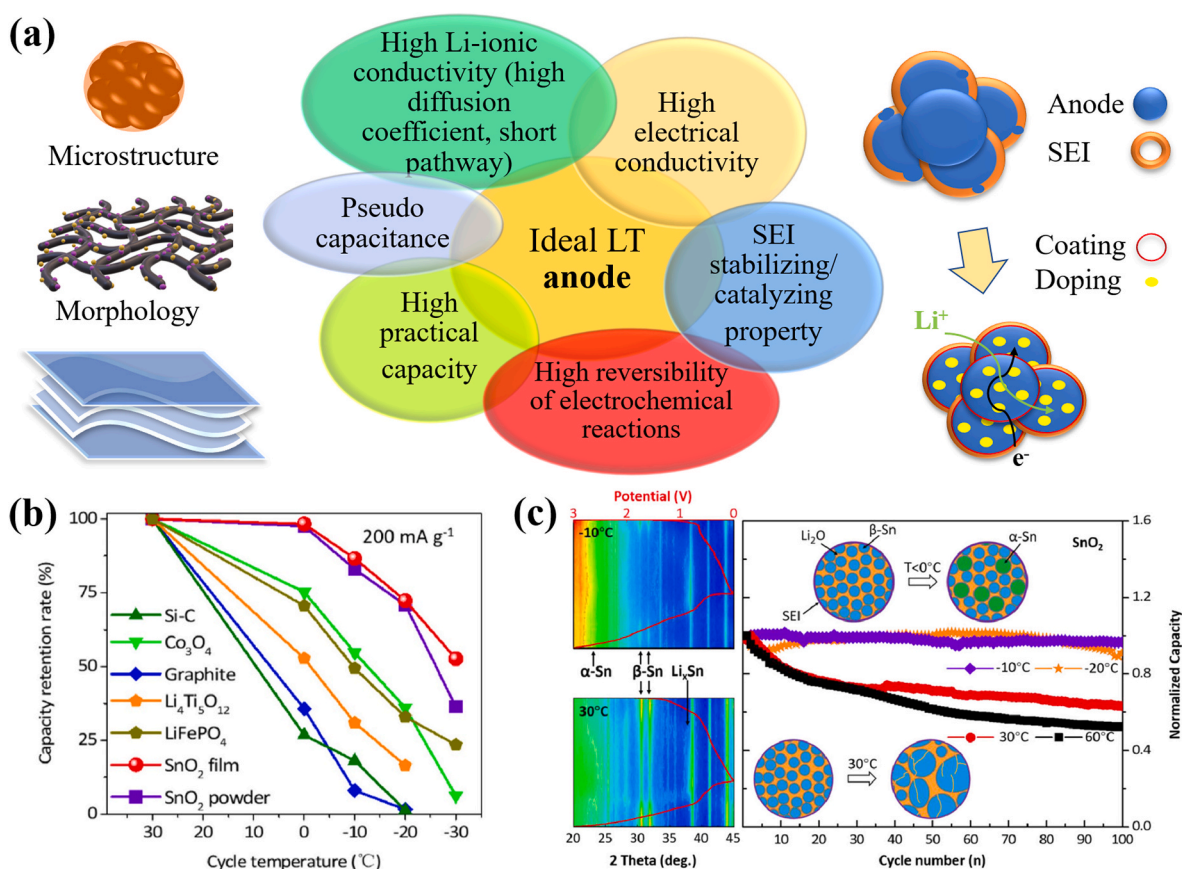


Fig. 3. (a) Main characteristics of anode materials with improved LT properties and corresponding approaches. (b) Capacity retention ratio of different materials at different temperatures and (c) mechanism of the improved electrochemical stability of  $\text{SnO}_2$  anode at low temperature. (Reproduced with permission from Ref. [55]. Copyright 2021, Elsevier).

**Table 1**  
LT performance of LIBs with modified anodes.

Anode material	Electrolyte	LT performance	Ref.
<i>Carbon-based materials</i>			
Metal-oxidized graphite (Me = Au, Ag, Ni, Cu, Al, Sn)	1 M LiPF <sub>6</sub> in EC: DEC:DMC = 1:1:1	-30 °C, 80–93 mAh g <sup>-1</sup> at C/5 for Al, Cu, Sn.	[41]
Oxidized graphite/Cu composite	1 M LiPF <sub>6</sub> in EC: DEC:DMC = 1:1:1	-30 °C, 130 mAh g <sup>-1</sup> at C/3	[56]
Graphite/Sn composite	1 M LiPF <sub>6</sub> in EC: DEC:DMC = 1:1:1	-30 °C, 152 mAh g <sup>-1</sup> at C/5	[39]
Nano-Sn embedded in graphite	1 M LiPF <sub>6</sub> in EC: DMC = 1:1	-20 °C, 200 mAh g <sup>-1</sup> at 0.1C	[42]
Plate-like synthetic graphite KS-6	1 M LiPF <sub>6</sub> in EC: DEC = 3:7	-5 °C, 301.7 mAh g <sup>-1</sup> at 0.1 mAh cm <sup>-2</sup>	[38]
Multilayer graphene	1 M LiPF <sub>6</sub> in EC: DEC:DMC = 1:1:1	-30 °C, 130 mAh g <sup>-1</sup> at 0.05 A g <sup>-1</sup>	[57]
Structure-Controlled Graphene	1 M LiPF <sub>6</sub> in EC: EMC:MP = 20:60:20 v/v%	-40 °C, ≈154 mAh g <sup>-1</sup> at 0.01 A g <sup>-1</sup>	[58]
Co-doped Zn <sub>2</sub> SnO <sub>4</sub> -graphene-C	1 M LiPF <sub>6</sub> in EC: EMC:DMC = 1:1:1	-25 °C, 196 mAh g <sup>-1</sup> at 0.1C	[59]
<i>Titanium oxides</i>			
Nano LTO	1 M LiPF <sub>6</sub> in PC: DME = 1:1 (wt.%)	-30 °C, 83 mAh g <sup>-1</sup> at C/8	[60]
Carbon-coated LTO	1 M LiPF <sub>6</sub> in EC: DMC = 1:1	-20 °C, 120 mAh g <sup>-1</sup> at 1 C	[61]
LTO/Ag/CNT	0.75 M LiTFSI in 1,3-Dioxolane	-60 °C, 140 mAh g <sup>-1</sup> at 0.2C	[62]
W-doped LTO/brookite	1 M LiPF <sub>6</sub> in EC: DMC:EMC = 1:1:1	-20 °C, ~205 mAh g <sup>-1</sup> at 0.1 A g <sup>-1</sup>	[63]
Nb-doped LTO-TiO <sub>2</sub>	1 M LiPF <sub>6</sub> in EC: DEC:DMC = 1:1:1	-20 °C, 128.6 mAh g <sup>-1</sup> at 1 C	[40]
TiO <sub>2</sub> rutile	1 M LiPF <sub>6</sub> in EC: DEC:DMC = 1:1:1	-40 °C, 77 mAh g <sup>-1</sup> at C/5	[46]
N-doped TiO <sub>2</sub> NT/TiN/graphene	1 M LiPF <sub>6</sub> in EC: DMC = 1:1	-20 °C, ~150 mAh g <sup>-1</sup> at 1 A g <sup>-1</sup>	[64]
<i>Other intercalation materials</i>			
Nb <sub>16</sub> W <sub>5</sub> O <sub>55</sub>	1 M LiPF <sub>6</sub> in EC: DEC = 1:1	-20 °C, 163 mAh g <sup>-1</sup> at 20 mA g <sup>-1</sup>	[65]
Fe <sub>2</sub> (MoO <sub>4</sub> ) <sub>3</sub> -HMS	1 M LiPF <sub>6</sub> in EC: DMC = 1:1 + 5 wt% FEC	-20 °C, 281 mAh g <sup>-1</sup> at 1 A g <sup>-1</sup>	[66]
Fe-added Fe <sub>3</sub> C carbon nanofibers	1 M LiPF <sub>6</sub> in EC: EMC:DMC = 1:1:1	-15 °C, 250 mAh g <sup>-1</sup> at 400 mA g <sup>-1</sup>	[67]
Fe <sup>3+</sup> -stabilized Ti <sub>3</sub> C <sub>2</sub> T <sub>x</sub> MXene	1 M LiPF <sub>6</sub> in EC: DEC = 1:1	-10 °C, 135.2 mA h g <sup>-1</sup> , 300 cycles, 200 mA g <sup>-1</sup>	[44]
<i>Alloying materials</i>			
Si	1 M LiPF <sub>6</sub> in FEC: DMC = 1:4	-30 °C, 600 mAh g <sup>-1</sup> at 1C	[50]
Ge nanowires	1 M LiPF <sub>6</sub> in EC: DEC:DMC = 1:1:1	-50 °C, 255 mAh g <sup>-1</sup> at 1 C	[68]
Ge	1 M LiPF <sub>6</sub> in EC: DEC = 1:1 + 3 wt % VC with 0, 10, 30, and 50 wt % PC	-20 °C, 1207 mAh g <sup>-1</sup> , 1 C, 90.42% retention, 400 cycles	[69]
3D porous Cu-Zn	1 M LiPF <sub>6</sub> in EC: DEC:DMC = 1:1:1	-20 °C, 197 mAh g <sup>-1</sup> and -30 °C, 137 mAh g <sup>-1</sup> at 0.1 A g <sup>-1</sup>	[70]
Nanoporous Cu-Ge-Al	1 M LiPF <sub>6</sub> in EC: DMC = 1:1	-20 °C, 122.9 mAh g <sup>-1</sup> at 1.0 A g <sup>-1</sup>	[71]
<i>Conversion-based materials</i>			
Ag-incorporated Fe <sub>2</sub> O <sub>3</sub> /CNF	1 M LiPF <sub>6</sub> in EC: EMC:DMC = 1:1:1	-5 °C, 560 mAh g <sup>-1</sup> at 600 mA g <sup>-1</sup>	[72]
Fe <sub>3</sub> O <sub>4</sub> nanorods in N-doped carbon mat	1 M LiPF <sub>6</sub> in EC: EMC:DMC = 1:1:1	17 ± 2 °C, 760 mAh g <sup>-1</sup> at 1000 mA g <sup>-1</sup> , 900 cycles	[73]
2D NiO@C-N Nanosheets	1 M LiPF <sub>6</sub> in EC: DMC = 1:1	-40 °C, 428 mAh g <sup>-1</sup> at 0.05 A g <sup>-1</sup>	[45]
Co <sub>3</sub> O <sub>4</sub> @graphene Composite	1 M LiPF <sub>6</sub> in EC:PC: EMC = 1:1:2 + 5 wt % FEC	-20 °C, ~450.2 mAh g <sup>-1</sup> at 0.5 A g <sup>-1</sup>	[74]
SnO <sub>2</sub> film	1 M LiPF <sub>6</sub> in EC:PC: EMC = 1:1:2 + 5 wt % FEC	-20 °C, 603.1 mAh g <sup>-1</sup> , -30 °C, 423.8 mAh	[55]

**Table 1 (continued)**

Anode material	Electrolyte	LT performance	Ref.
SnO <sub>2</sub> -LiF-graphite	1 M LiPF <sub>6</sub> in EC:PC: EMC = 1:1:2 + 5 wt % FEC	g <sup>-1</sup> , 100 cycles, at 200 mA g <sup>-1</sup> -40 °C, 780.4 mAh g <sup>-1</sup> and -50 °C, 637.2 mAh g <sup>-1</sup> at 100 mA g <sup>-1</sup>	[75]
Cauliflower-Like CoFe <sub>2</sub> O <sub>4</sub>	1 M LiPF <sub>6</sub> in EC: DMC = 1:1	-25 °C, 664.5 mAh g <sup>-1</sup> at 100 mA	[76]
VS <sub>4</sub>	1 M LiPF <sub>6</sub> in EC: DMC:DEC	-20 °C, 259.6 mAh g <sup>-1</sup> at 100 mA g <sup>-1</sup>	[77]
FeS	1 M LiPF <sub>6</sub> in EC: DMC = 1:1	-20 °C, 562 mAh g <sup>-1</sup> at 0.2 A g <sup>-1</sup>	[78]
MoS <sub>2</sub> /Carbon	1 M LiPF <sub>6</sub> in EC: DMC = 1:1	-20 °C, 854.3 mAh g <sup>-1</sup> , 100 mA g <sup>-1</sup>	[79]
N-doped C/a-MnS/flake graphite	1 M LiPF <sub>6</sub> in EC: DEC = 1:1	-20 °C, 350 mAh g <sup>-1</sup> , 50 cycles, 100 mA g <sup>-1</sup>	[80]
Cu <sub>2</sub> ZnSnS <sub>4</sub>	1 M LiPF <sub>6</sub> in EC: EMC:DMC = 1:1:1	-10 °C, 475 mAh g <sup>-1</sup> , 200 cycles, 500 mA g <sup>-1</sup>	[81]
Coral-Like Fe <sub>7</sub> Se <sub>8</sub> @C	1 M LiPF <sub>6</sub> in PC:EC + 5 wt% FEC	-25 °C, 710.3 mAh g <sup>-1</sup> at 0.1C	[82]

materials is to insert electrochemically inactive components in a small proportion. It was established that the intermetallic alloy material could be applied to solve the problem of volume change of the alloy anodes [84]. During charging and discharging, active compounds of intermetallic material interact with Li<sup>+</sup> at various potentials, while inactive compounds keep the structural stability and high electrical conductivity, thus enhancing the performance of the anode [85]. Eventually, de-alloying the intermetallic compounds can overcome two LT issues: increasing electrical conductivity and integrating volume changes of alloying anodes [71]. However, it compromises the overall capacity.

*Conversion-based materials* (pure conversion, combined conversion-alloying, and conversion-intercalation type), such as metal oxides, sulfides, and selenides (e.g., NiO, MoS<sub>2</sub>, Fe<sub>7</sub>Se<sub>8</sub>), are getting more attention as alternatives to graphite due to their availability, high theoretical capacities, and lower volume expansions during lithiation compared to alloying materials [45,72,77,82,86]. Furthermore, after the extensive studies on the LT performance of different conversion materials, it was found that they can deliver higher capacities at subzero temperatures, exceeding the capacity of LTO and alloying materials under the same LT conditions [74]. Sn-based materials as anode show stable capacity retention for long cycles at low temperatures. Taking conversion-alloying type SnO<sub>2</sub> as an example, Tan et al. attributed it to the improved structural stability and reversibility of lithiation reactions in pure SnO<sub>2</sub> electrodes by lowering the temperature due to unique allotropic changes of Sn [55]. The main limitation of metal oxides is low electrical conductivity and high SEI resistance at low temperatures [45, 75].

While the commercialization of most alternative anode materials remains questionable, studies on the commercial anode-electrolyte interactions at low operating temperatures seem more practical.

### 3.2.2. Morphology and structure

Another method of enhancing the LT performance of anode is to use various nanomaterials (nanoparticles, thin films, nanowires, nanotubes, nanofibers, core-shell, and yolk-shell structures, and so on). Gavrilin et al. focused on designing 1D structures, namely nanowires and the study showed that even at -50 °C, the Ge nanowire anode revealed a capacity of about 255 mAh g<sup>-1</sup> [68]. It was found that nanowires (nanotubes and nanofibers) provide good electrical conductivity along their length, short lithium-ion diffusion pathway, and more contact area between electrolyte and electrode materials [64,67,72].

Bai et al. have prepared 2D nickel oxide nanosheets coated with N-

doped carbon layer composite and applied as an anode for LIBs [45]. The batteries had excellent electrochemical properties in a wide range of temperatures (from room temperature to  $-40^{\circ}\text{C}$ ). A hierarchical porous 2D structure improves the contact area between electrode materials and electrolytes, providing much more available insertion sites for lithium and enhancing the electrochemical performance [63].

The 3D structure can accelerate the process of electron transfer and shorten the diffusion and migration pathways of  $\text{Li}^+$  [87]. Due to their interconnected channels for electrolyte permeation, porous metallic structures have faster  $\text{Li}^+$  transportation, and accommodation of (de) lithiation-accompanied volume changes. For example, Yu et al. proposed strategies to overcome the volume expansion effects and improve the conductivity of  $\text{VS}_4$  [77]. They have prepared a 3D nest-like microstructure for modification of  $\text{VS}_4$  anode. As a result, this approach shows excellent LT electrochemical performance and even remains  $259.6\text{ mAh g}^{-1}$  at  $100\text{ mA g}^{-1}$  at subzero  $20^{\circ}\text{C}$ . Similarly, 3D nanoporous alloy anodes can also increase electrochemical performance at low temperatures [71]. To overcome the problem of restacking graphene anode material, different 3D nanostructures are introduced. For example, aerogel, folded form, 3D nano- and macro-porosity, and laser-scribed graphene anodes. Such structures can provide a larger surface area with electrochemical activity and superior performance at LT conditions. This can be explained by the adsorption of  $\text{Li}^+$  on the defect sites of modified graphene. These findings have opened a way for developing 3D structure-controlled anodes, as it lets the battery operate at extremely low temperatures ( $-40^{\circ}\text{C}$ ) [58].

The significant slowdown of the diffusion-controlled charge storage mechanism of intercalation-type anodes limits their LT performance fundamentally. In contrast to diffusion-controlled batteries, supercapacitors with the temperature-independent surface-controlled energy storage mechanism show better LT performance due to rapid  $\text{Li}^+$  intercalation/de-intercalation on the electrochemical double-layer even at low temperatures [58]. Therefore, recent works focused on improving the pseudocapacitive properties of anode materials by controlling the morphology or surface defects and introducing the additional surface-controlled energy storage mechanism [45,73,81]. Such pseudocapacitive behavior can significantly improve the lithium storage capacity, cycling stability, and rate capability of anode materials at low temperatures [45,76,80]. Furthermore, control of the morphology and structure is admitted to comprehensively address the main LT limitations of the anode materials by affecting the conductivity of electrons, pathlength of the  $\text{Li}^+$ , and contact area of the electrode with electrolyte, thus number of electrochemically active sites [28,57,58,63,64,68]. For example, structure-controlled graphene anode with surface defect sites demonstrates excellent LT performance (capacity of  $\approx 154\text{ mAh g}^{-1}$  at  $0.01\text{ A g}^{-1}$ ) and outstanding cycling stability at a temperature of  $-40^{\circ}\text{C}$  [57]. On the other hand, excessive reactivity of the electrolyte with the anode, leading to side reactions, may be a significant drawback of applying nanostructures.

### 3.2.3. Coating and doping

Coating and doping are other practical approaches to enhance the conductivity of electrons and ions and affect the SEI layer formation in the LT anode materials [40,59,63,67]. Such modifications reduce the charge/discharge resistance and enhance the  $\text{Li}^+$  intercalation, as the appropriate changes in the surface chemistry of the anode lead to the formation of a stable SEI layer of high ionic conductivity [44,56]. Furthermore, metal coating on carbon anodes, such as Sn coating by vapor deposition, is believed to catalyze the anion desolvation and enhance the internal conductivity of the bulk electrode [39].

Gao et al. doped Co into  $\text{Zn}_2\text{SnO}_4$ -graphene-carbon nanocomposite, and it significantly decreased the  $R_{\text{ct}}$  and improved the cyclic performance [59]. Doping of  $\text{Nb}^{5+}$  into  $\text{TiO}_2$ -coated LTO led to a partial reduction of  $\text{Ti}^{4+}$  to  $\text{Ti}^{3+}$ , improving the conductivity and expanding the crystal lattice to increase the lithium-ion diffusion coefficient [40]. On the other hand,  $\text{W}^{6+}$  doping into semiconducting LTO/ $\text{TiO}_2$  composite

improved the electrical conductivity by decreasing the band gap value and helping to lower the polarization [63].

Zou et al. incorporated Ag into  $\text{Fe}_2\text{O}_3$  carbon nanofibers, which facilitated electron conduction, maintained the structural integrity of active materials, enhancing charge-transfer efficiency and lithium diffusion coefficient at low temperatures [72]. The same group added Fe into  $\text{Fe}_3\text{C}$  carbon nanofibers, and it not only improved the electrical conductivity but also catalyzed the reduction of some SEI components [67]. As a result, at a low temperature of  $-15^{\circ}\text{C}$ , the composite had a capacity of  $250\text{ mAh g}^{-1}$  at  $400\text{ mA g}^{-1}$  even after 55 cycles.

To solve the low  $\text{Li}^+$  diffusion problem and stabilize the SEI layer,  $\text{Ti}_3\text{C}_2\text{T}_x$  MXene anode was doped by  $\text{Fe}^{3+}$  ions [44]. The  $\text{Fe}^{3+}$ -stabilization made  $-\text{O}/-\text{OH}$  groups in MXene interlayers active towards  $\text{Li}^+$  and lowered the diffusion barrier. The material showed stable cyclability with  $135.2\text{ mAh g}^{-1}$  capacity after 300 cycles under the current density of  $200\text{ mA g}^{-1}$  at  $-10^{\circ}\text{C}$ .

Doping nonmetals, such as N, also effectively improves the LT performance by enhancing the electrical conductivity of anode materials [64].

### 3.2.4. Electrode composition

Electrodes are usually composed of anode active material, conductive carbon black, and binder coated on the Cu foil current collector. The conductive carbon black in the electrode guarantees good contact between the active material particles and compensates for the reduced electrical conductivity caused by the addition of low-conductive binders. The content of the carbon black in the electrode may vary from 3 to 20 wt% depending on the conductivity of the active material. Additional modifications on the carbon black were also proposed to increase the overall conductivity of the electrodes further. For instance, Marinaro et al. proposed replacing pristine Super-P with a Cu/Super-P composite as a conductive agent to improve the overall conductivity and LT performance of the LTO anode [88]. As a result of enhanced ionic and electronic transport in the electrode after Cu addition, the capacity at  $-30^{\circ}\text{C}$  improved from 95 to  $131\text{ mAh g}^{-1}$  at 0.2C.

Properties of binders, such as the adhesion strength, glass transition temperature ( $T_g$ ), ionic conductivity, and electrolyte absorption, also play a vital role in the LT performance of the electrode. Even though sodium salt of carboxymethyl cellulose (CMC) and styrene-butadiene rubber (SBR)/CMC have the higher mechanical strength to accommodate the volume expansion during cycling, studies have shown that anode materials with poly(vinylidene fluoride) (PVDF) binder possess faster  $\text{Li}^+$  diffusion at low temperatures due to higher electrical and ionic conductivity of PVDF [35]. To improve the adhesion of the PVDF-containing electrode material to the current collector, the surface oxides of the Cu foil are sometimes etched by the oxalic acid added to the slurry [35,39,41,56].

The preparation of binder-free electrodes could eliminate the additional resistance coming from the binder. Thus, active materials deposited on substrates or vacuum-filtrated free-standing electrodes were directly used without any coating procedure [58,68,70]. Tan et al. compared LT properties of binder-free  $\text{SnO}_2$  film (sputtered onto Cu foil) to that of conventional  $\text{SnO}_2$  electrodes (prepared by slurry method), and the binder-free film showed improved rate-capability at  $-10^{\circ}\text{C}$  and higher retention of the room-temperature capacity of 52.6% at  $200\text{ mA g}^{-1}$  (vs. 37.5% for conventional  $\text{SnO}_2$  electrodes) at  $-30^{\circ}\text{C}$  [55].

## 4. Cathodes

### 4.1. Challenges in cathodes at low temperatures

After studying electrical characteristics of 18,650 Li-ion cells at low temperatures, Nagasubramanian concluded that the main reason for poor cell performance can be an increased resistance from CEI [89]. The unstable surface of the active material of cathode and side reactions on CEI caused by high overpotential can also influence the impedance level,



therefore leading to capacity loss and battery cycling life shortage [90–92]. Direct contact of the cathode with the electrolyte on the CEI-free surfaces may lead to the dissolution of transition metals (TMs) and their deposition on the anode or separator, causing a capacity decrease [93,94]. TM ions play an essential role as the rapid redox reaction centers, and their dissolution rate usually increases with temperature. Although low temperature should inhibit the dissolution of TM, increased heat generation due to the increased internal resistance of the battery at low temperature can give a reverse effect, especially under extreme conditions [95]. Moreover, unlike temperatures above 0 °C, in some studies, more severe loss of the active cathode material and faster performance degradation were observed at lower discharging rates (0.5C) compared to higher ones (1 and 2 C) at –10 °C [96,97]. Another factors contributing to the capacity loss of the cathode at LT are reduced activation of the material, poor Li<sup>+</sup> intercalation, and the lattice crystal construction, limiting the diffusion of ions [13,32].

#### 4.2. Approaches to improve performance of cathodes at low temperatures

Sometimes the capacity of LIBs at low temperatures can be enlarged up to about 10% by simply increasing the charging cut-off voltage. On the other hand, the changed cut-off voltage should not exceed the tipping point, at which irreversible oxidation of the electrolyte and a rapid loss of the active material start [98].

Since layered LiCoO<sub>2</sub>-based cathode materials are more vulnerable to LT operations due to corrosions from HF and poor stability of the surface structure [14,99], alternative cathode materials and their modifications, including olivine LiFePO<sub>4</sub> (LFP), layered LiNi<sub>x</sub>Co<sub>y</sub>Mn<sub>z</sub>O<sub>2</sub> (NCM), and spinel LiMn<sub>2</sub>O<sub>4</sub> (LMO), have been extensively studied. Table 2 summarizes the LT performance of LIBs with modified cathodes.

Consecutive engineering methods for cathode materials improve LT performance. These methods deliberately modify the cathode active material to make their lithiation and delithiation processes at low ambient temperatures more kinetically stable. The main modification methods are surface coating, metal doping, and particle size reduction. Surface coating improves the surface conductivity of cathode material, reduces contact resistance, and prevents the dissolution of TMs [100]. Metal doping promotes the mobility of Li<sup>+</sup> and electrons in the material by forming vacancies in the lattice structure and broadening the ion diffusion channel [101]. Furthermore, it stabilizes the CEI layer, preventing the side reactions with electrolytes and suppressing the

dissolution of transition metals. Particle size reduction significantly shortens the diffusion path distance of Li<sup>+</sup> and facilitates the lithium insertion/extraction process [102].

##### 4.2.1. Olivine LFP cathode materials

LFP is considered a promising cathode material owing to its moderate theoretical capacity (170 mAh g<sup>-1</sup>), low cost, eco-friendliness, and natural abundance of iron. Furthermore, the oxygen release would not happen due to the strong P–O bond, which guarantees the robust structure and thermal stability during charging and discharging [103, 104]. The main drawbacks of LFP at low temperatures include poor electrical conductivity, low Li<sup>+</sup> diffusion coefficient, and sluggish Li<sup>+</sup> migration rate during discharge, originating from their constricted ion transportation in one dimension (1D) along the b-axis (Fig. 4a) [101]. Therefore, the main improvement approaches are directed toward overcoming these limitations.

The coating materials used to improve the electronic and ionic conductivities of the LFP cathode can be classified as carbon-based (e.g., Ketjen black, carbon nanotubes, and P-doped carbon) [100,105,106], organic (conductive polymers, e.g., polypyrrole) [108], and inorganic (e.g., LTO) [109]. The application of such coatings improves the diffusion of Li<sup>+</sup> in the solid phase and, at the same time, helps to enhance the bulk conductivity of the nanocomposite, forming an excellent conductive network (Fig. 4b). Furthermore, partially acting as an artificial CEI layer, it can protect from corrosion by preventing direct contact of electrolytes with Fe<sup>2+</sup> ions.

To further improve the LT properties of the LFP cathode, doping the carbon-coated material with rare-earth and metallic elements was also proposed [101]. These elements enhance the electronic conductivity and decrease the contact resistance by occupying the Li site.

The microstructure of the carbon-coated LFP plays another significant role in its LT performance. For example, due to the shortening of the Li<sup>+</sup> diffusion distance, LFP/C with a sheet structure and the pomegranate-like spherical structure, composed of smaller internal particles within a large particle, exhibited improved retention rates at –20 °C compared to one with a large spherical structure [107].

##### 4.2.2. Layered NCM cathode materials

LiNi<sub>x</sub>Co<sub>z</sub>Mn<sub>y</sub>O<sub>2</sub> (NCM) is one of the most extensively used cathode materials, owing to its high reversible capacity (250 mAh g<sup>-1</sup>), low environmental risks, and compared to other cathode materials, high Li<sup>+</sup>

**Table 2**  
LT performance of LIBs with modified cathodes.

Cathode materials	Electrolyte	LT performance	Ref.
<i>Olivine LFP</i>			
LFP/Ketjen Black	1 M LiPF <sub>6</sub> in EC:DMC = 1:1	–20 °C, 120.2 mAh g <sup>-1</sup> at 1 C	[105]
LFP/C–P	1 M LiPF <sub>6</sub> in EC:DMC:EMC = 1:1:1	–40 °C, 82.7 mAh g <sup>-1</sup> at 0.1C	[106]
LFP/C	1 M LiPF <sub>6</sub> in EC:DMC = 1:1	–20 °C, 89.3 mA h g <sup>-1</sup> at 0.5C (58.7%)	[107]
LFP@C/CNT	1 M LiPF <sub>6</sub> in EC:DMC:EMC = 1:1:1	–25 °C, 71.4% of initial 160 mAh g <sup>-1</sup> , 0.2C	[100]
LFP/PPy nanorod	1 M LiPF <sub>6</sub> in EC:DMC = 1:1	–20 °C, 128 mAh g <sup>-1</sup> at 0.1C	[108]
LTO coated SP-LFP/C	1 M LiPF <sub>6</sub> in EC:DEC = 1:1	0 °C, 45 mA h g <sup>-1</sup> at 0.5C	[109]
La <sup>3+</sup> Mg <sup>2+</sup> LFP/CA	1 M LiPF <sub>6</sub> in EC:DMC = 1:1	–20 °C, 120.3 mAh g <sup>-1</sup> at 1 C	[101]
V <sup>3+</sup> and F co-doped LFP/C	1 M LiPF <sub>6</sub> in EC:DMC = 1:1	0 °C, 86 mAh g <sup>-1</sup> at 10 C	[110]
Ti-doped LFP/C	1 M LiPF <sub>6</sub> in EC:DEC = 1:1	–20 °C, 122.3 mAh g <sup>-1</sup> at 1 C	[111]
<i>Layered NCM</i>			
NCM 111	1 M LiPF <sub>6</sub> in MP:FEC (90:10 vol %)	–20 °C, 111 mAh g <sup>-1</sup> at 0.5C	[112]
NCM 532	1 M LiTFSI <sub>0.6</sub> –LiTFFPB <sub>0.4</sub> in PC: EC:EMC = 1:1:3	–20 °C, 101.3 mA h g <sup>-1</sup> at 0.1C	[113]
NCM 622	LiPF <sub>6</sub> in EC:DEC	0 °C, 55 mAh g <sup>-1</sup> at 5 C	[114]
NCM 622	1 M LiPF <sub>6</sub> in EC:DMC:EMC = 1:1:1	–32 °C, 205 mAh at HL	[115]
NCM 71515	LiPF <sub>6</sub> EC:EMC:DMC = 1:1:1	–20 °C, 424472.41 W/m <sup>3</sup> at 2C	[116]
NCM 90	1.2 M LiPF <sub>6</sub> in EC:EMC = 3:7 v/v + 2 wt% VC	0 °C, 170 mAh g <sup>-1</sup> , 0.5C, 100 cycles	[117]
Co-free NM 90		0 °C, 140 mAh g <sup>-1</sup> , 0.5C, 100 cycles	
Ti surface-doped NCM	1 M LiPF <sub>6</sub> in EC:DMC:EMC = 1:1:1 vol.	–20 °C, 122.4 mAh g <sup>-1</sup> at 5 C	[118]
AlF <sub>3</sub> -coated Li <sub>1.2</sub> Ni <sub>0.13</sub> Co <sub>0.13</sub> Mn <sub>0.54</sub> O <sub>2</sub>	1 M LiPF <sub>6</sub> in EC:DMC = 1:1	–20 °C, 109.3 mAh g <sup>-1</sup> at 0.1C	[119]
<i>Spinel LMO</i>			
Al-doped LMO/acid-treated Super P	1.15 M LiPF <sub>6</sub> in EC:DMC:EMC = 3:4:3	–10 °C, 75 mAh g <sup>-1</sup> at 100 C	[120]
LMO with SiO <sub>2</sub> as separator	LiPF <sub>6</sub> in EC:DEC = 1:1 w/w	–20 °C, 92.3 mAh g <sup>-1</sup> at 0.2C	[121]
LMO-MST	1 M LiPF <sub>6</sub> in EC:DMC:EMC = 1:1:1 vol.	–5 °C, 123.9 mAh g <sup>-1</sup> at 0.5C	[102]

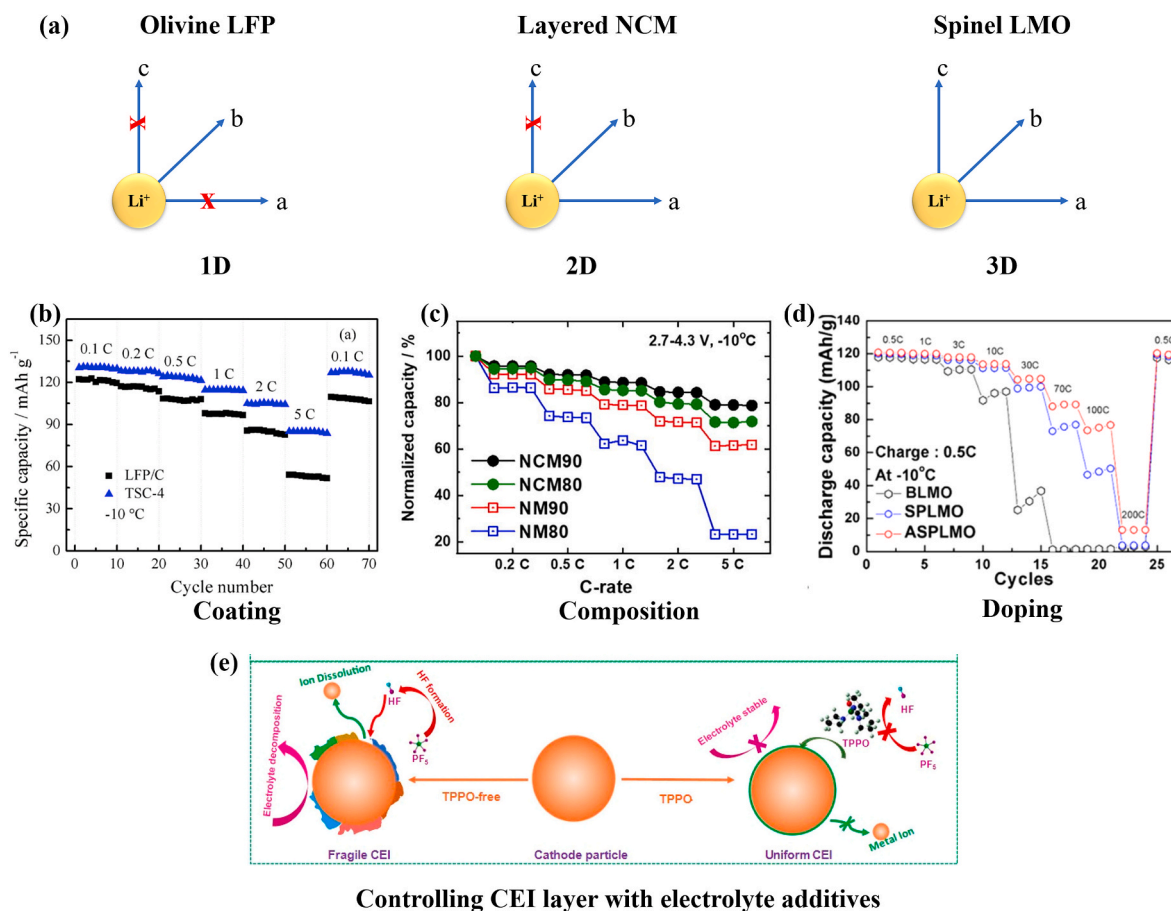


**Fig. 4.** (a)  $\text{Li}^+$  diffusion directions in cathode materials of different structures. (b) Rate performance of the  $\text{Ti}_3\text{SiC}_2$ -modified and pristine LFP/C cathode materials at  $-10^\circ\text{C}$ . (Reproduced with permission from Ref. [122]. Copyright 2015, Elsevier). (c) Rate capabilities of NM and NCM cathodes with increasing current density cycled at  $-10^\circ\text{C}$ . (Reproduced with permission from Ref. [123]. Copyright 2022, Elsevier). (d) The discharge rate capability of  $\text{Al}^{3+}$ -doped and pristine LMO electrodes at  $-10^\circ\text{C}$ . (Reproduced with permission from Ref. [120]. Copyright 2017, American Chemical Society). (e) Schematic of the interfacial chemistry in different electrolytes. (Reproduced with permission from Ref. [124]. Copyright 2021, American Chemical Society).

diffusivity, which makes it promising for LT usage. Compared with LFP, the  $\text{Li}^+$  diffuses along a 2D channel perpendicular to the c-axis in NCM (Fig. 4a). Instead of two phases, such as in LFP, layered TM oxides exhibit a single-phase solid solution during reversible lithiation/delithiation [123]. The electrostatic interaction of TM cations on  $\text{Li}^+$  influences the work done by the system to transfer  $\text{Li}^+$ . Consequently, the  $\text{Li}^+$  diffusion kinetics depend on the Li slab space and the type and valence state of TMs. Current research on LT capacity performance of NCM cathode mainly focuses on the increased diffusion kinetics of  $\text{Li}^+$  by controlling the ratio of three metal ions (Ni, Co, Mn). Different types of NCM cathode materials with different ratios of Ni, Co, and Mn was engineered and studied:  $\text{Li}(\text{Ni}_{1/3}\text{Mn}_{1/3}\text{Co}_{1/3})\text{O}_2$  (111) [112],  $\text{Li}(\text{Ni}_{0.4}\text{Mn}_{0.4}\text{Co}_{0.2})\text{O}_2$  (442) [125],  $\text{Li}(\text{Ni}_{0.5}\text{Mn}_{0.3}\text{Co}_{0.2})\text{O}_2$  (532) [113],  $\text{Li}(\text{Ni}_{0.6}\text{Mn}_{0.2}\text{Co}_{0.2})\text{O}_2$  (622) [114,115],  $\text{Li}(\text{Ni}_{0.7}\text{Mn}_{0.15}\text{Co}_{0.15})\text{O}_2$  (71515) [116], and  $\text{Li}[\text{Ni}_{0.9}\text{Co}_{0.1}]\text{O}_2$  (NC90),  $\text{Li}[\text{Ni}_{0.9}\text{Co}_{0.05}\text{Mn}_{0.05}]\text{O}_2$  (NCM90), and  $\text{Li}[\text{Ni}_{0.9}\text{Mn}_{0.1}]\text{O}_2$  (NM90) [117]. Their wide variety and a large amount of information collected open the way to further study their LT properties. Among different NCM materials, NCM622 has the highest  $\text{Li}^+$  diffusion coefficient, with the minimum temperature change in the temperature range from  $-25$  to  $50^\circ\text{C}$  [114]. Even though increasing the Ni content in NCM allows for higher capacities at room temperatures, Co plays an important role in maintaining its high electrical conductivity and LT performance (Fig. 4c) [117].

#### 4.2.3. Spinel LMO cathode materials

The spinel  $\text{LiMn}_2\text{O}_4$  (LMO) cathode materials have many advantages (high power, low cost, favorable safety, and environmental

friendliness). Compared to the other two types of cathodes mentioned above, it has a 3D structure advantageous for fast  $\text{Li}^+$  diffusion (Fig. 4a). However, it suffers from the increased cell impedance and low charging efficiency from regenerative braking at low temperatures [120]. The main approaches for improving the LT properties of LMO are directed to the suppression of the manganese dissolution. Xu et al. improved the stability of LMO by controlling its morphology [102]. The unique sphere-bridged tube jointless outer structure and the most exposed stable facets on the surface of the crystals prevented the dissolution of manganese ions, and the LMO cathode maintained optimal cycling performance at  $-5^\circ\text{C}$ . Chen et al. proposed to trap HF, which accelerates the dissolution of manganese ions, by implementing a porous silicon dioxide ( $\text{SiO}_2$ ) separator [121]. Along with the suppression of the manganese dissolution, the electrolyte-infiltrated separator demonstrated high ionic conductivity of  $0.35\text{ mS cm}^{-1}$  due to its hydrophilic properties, high porosity, and excellent mechanical strength at  $-20^\circ\text{C}$ . As a result, LMO cells with this separator exhibited improved capacity and stability at low operating temperatures.

## 5. Electrolytes

### 5.1. Role of electrolyte on the formation of interphasal films on electrodes

#### 5.1.1. SEI layer formation at low temperatures

The formation of the SEI layer is inevitable on the anode materials because their lithiation potential lies outside the thermodynamic stability window of the typical organic electrolytes [126]. The primary



mechanism of SEI formation occurs during the oxidation and reduction of the electrolyte at the electrode surface during the first few charge-discharge cycles. However, low temperatures affect the formation of a stable film on the electrode surface and significantly reduce the performance of LIBs. Large amounts of  $\text{Li}^+$  are consumed in the first cycle, forming a relatively dense SEI at low temperatures due to lower solubility and worse kinetic characteristics of  $\text{Li}^+$ , leading to large polarization and low efficiency [48,127].

The formation and properties of SEI films largely depend on the composition of the electrolyte [128–130]. The addition of SEI-forming additives or co-solvents to the electrolyte solution is believed to be a practical approach to improving the LT properties of LIBs [131–133]. For example, moderate amounts of functional additives, such as prop-1-ene-1,3-sultone (PES) and lithium difluorobis(oxalato) phosphate (LiDFBOP), promoted the formation of highly conductive SEI films with low resistance [131,132]. However, the effectiveness of the

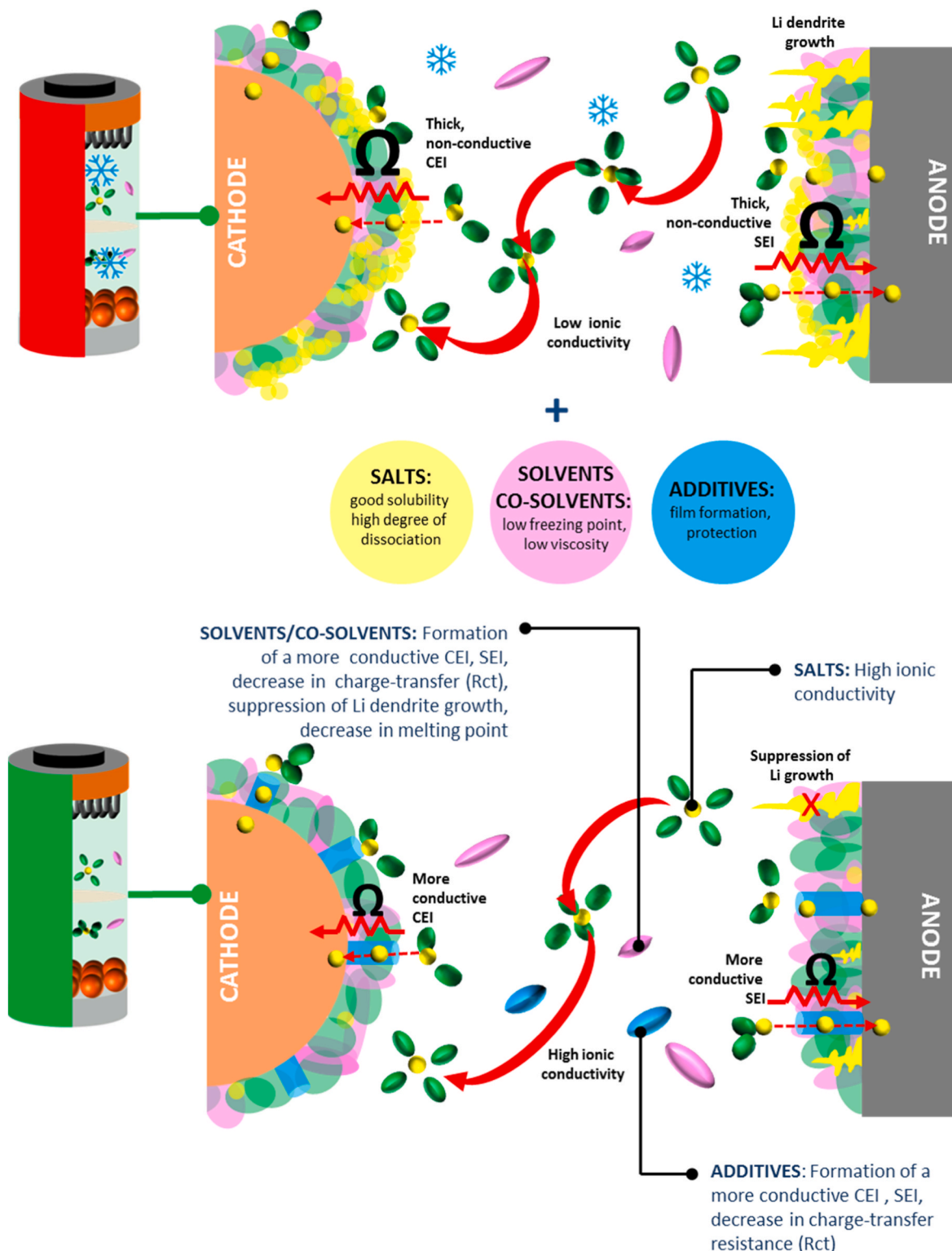


Fig. 5. Performance enhancement of LIBs at low temperatures from an electrolyte perspective.

additives strongly depends on the temperature. For example, with the addition of 10 wt% vinylene carbonate (VC), one of the well-known SEI layer forming additives at high temperatures, to the cell with Si anode, at  $-5\text{ }^{\circ}\text{C}$ , the discharge capacity considerably deteriorated due to poor ionic and electrical conductivity of the SEI layer [134]. Thus, to optimize the electrolyte for LT applications, it is necessary to balance the intrinsic physical properties of the formulations (i.e., freezing point, viscosity, and ionic conductivity) with the observed compatibility with the selected cell chemistry (i.e., the nature of the passivation film formed on the electrodes) at low operating temperatures.

### 5.1.2. CEI layer formation at low temperatures

The CEI layer has a crucial role in increasing the surface stability of the cathode because of the effective suppression of the electrolyte decomposition at the electrolyte/electrode interface, preventing the transfer of electrons between electrode and electrolyte [135–138]. On the other hand, low temperature compromises the formation of a uniform CEI layer, degrading the LT performance of cathode in electrolytes without any functional additives (Fig. 4e) [124].

The formation of a fragile CEI at low temperatures leads to its overgrowth, irreversibly consuming  $\text{Li}^+$  from the electrolyte. It, in turn, decreases the concentration of  $\text{Li}^+$  in the electrolyte and increases the cell impedance, causing severe performance degradation [139,140]. Controlling the electrolyte composition to form a thin and uniform  $\text{LiF}$ -rich CEI layer on the surface of the cathode is believed to improve its  $\text{Li}^+$  conductivity and suppress the dissolution of TMs [112]. Furthermore, it reduces the  $R_{\text{ct}}$  and comprehensively improves the LT performance of the cathode.

Due to high complexity and only recent interest in the subject, these processes are poorly researched but should be studied in more detail in the future to fully assess the impact of the low temperature on the cathode performance.

## 5.2. Approaches to improve performance of electrolytes at low temperatures

To improve the poor performance of LIBs at sub-zero temperatures, the modification and development of electrolytes are essential. The addition of additives, co-solvents and salts, ionic liquids to the electrolyte, and changing the ratio of the electrolyte composition is mainly aimed at lowering the freezing point, lowering the viscosity, increasing the ionic conductivity, and forming SEI and CEI passivation layers with reduced resistance at low temperatures as seen in Fig. 5. Table 3 summarizes various modified LT electrolytes studied in different cell configurations.

### 5.2.1. Solvent modification

The main approaches to solvent modification include using various compositions and ratios of organic carbonates, making fluorinated electrolytes, using organic esters and other organic co-solvents. In general, the commercial electrolyte of LIBs is an anhydrous solution that consists of  $\text{LiPF}_6$  salt dissolved in organic carbonates. The studied solvent mixtures mainly consist of two or more organic carbonates, such as ethylene carbonate (EC), ethyl methyl carbonate (EMC), dimethyl carbonate (DMC), diethyl carbonate (DEC), and propylene carbonate (PC), with different physical and chemical properties. However, LIBs with conventional commercial carbonate-based electrolytes lose most of their capacity at low temperatures [4]. The freezing point of a commercial electrolyte consisting of 1 M  $\text{LiPF}_6$  in 1:1 EC:DMC is about  $-30\text{ }^{\circ}\text{C}$ . Many exciting approaches toward solvent modification have been used to improve and develop LT electrolytes.

One of the approaches is adding co-solvents with lower freezing points. For example, Plichta and Behl used EMC ( $-55\text{ }^{\circ}\text{C}$ ) as a co-solvent to increase the liquidus range of commercial EC:DMC electrolyte, so the cell with modified electrolyte can work at low temperatures down to  $-40\text{ }^{\circ}\text{C}$  [4]. Another approach is reducing the viscosity of the electrolyte

**Table 3**

LT performance of LIBs with modified electrolytes.

Electrolyte	System	LT performance	Ref.
<i>Solvent modification</i>			
1 M $\text{LiPF}_6$ in EC:EMC:TFENCH = 6:24:10	LCO/graphite	$-35\text{ }^{\circ}\text{C}$ , 20 cycles, -	[141]
1 M $\text{LiPF}_6$ in DMC:EMC = 3:5 + BA16% + EC10%	NCM811/Li	$-40\text{ }^{\circ}\text{C}$ , 60.5% of its RT capacity, 50 cycles	[142]
1 M $\text{LiPF}_6$ in MTFP/FEC = 9:1	NCM811/Li	$-60\text{ }^{\circ}\text{C}$ , 133 mAh $\text{g}^{-1}$	[143]
1 M $\text{LiPF}_6$ in EC:DEC = 1:2 + 28.6% EP	LCO/graphite	$-20\text{ }^{\circ}\text{C}$ , 186 mAh $\text{g}^{-1}$	[144]
0.75 M $\text{LiPF}_6$ in EC:DEC:DMC:EB = 1:1:1:1	graphite/Li	$-20\text{ }^{\circ}\text{C}$ , 292 mAh $\text{g}^{-1}$	[145]
1 M $\text{LiPF}_6$ in PC:EC:MB	LCO/graphite	$-30\text{ }^{\circ}\text{C}$ , 95 mAh $\text{g}^{-1}$ , C/2	[146]
1 M $\text{LiPF}_6$ in EC:DEC:FEC = 4.5:4.5:1	Si@graphite@C/Li	$-5\text{ }^{\circ}\text{C}$ , 2300 mAh $\text{g}^{-1}$	[134]
1 M $\text{LiPF}_6$ in EC:DEC:DMC:EMC = 1:1:1:3	$\text{LiNi}_x\text{Co}_{x-1}\text{O}_2$ /MCMB	$-50\text{ }^{\circ}\text{C}$ , 68.9% retention, 0.1C	[147]
<i>Modification of lithium salt</i>			
1 M $\text{LiPF}_6$ in EC:EMC:PC = 4:7:1 + 1% $\text{LiPO}_2\text{F}_2$	NCM523/graphite	$-20\text{ }^{\circ}\text{C}$ , 91.7 mAh $\text{g}^{-1}$ , 100 cycles	[148]
0.4 M $\text{LiDFOB/LiBF}_4$ (1:1) in EC:DEC:DMS = 1:2:1	LFP/Li	$-40\text{ }^{\circ}\text{C}$ , 82.5 mAh $\text{g}^{-1}$ , 55.7% retention	[149]
<i>Additives</i>			
1 M $\text{LiPF}_6$ in EC:EMC = 1:2 + 1% EMI- $\text{BF}_4$	NCM523/graphite	$-30\text{ }^{\circ}\text{C}$ , 878.7 mAh, 0.5C $-10\text{ }^{\circ}\text{C}$ , 150 cycles, 89.4% retention	[150]
1 M $\text{LiPF}_6$ in EC:EMC = 1:2 + 1.0% PFPMS	NCM523/graphite	$-20\text{ }^{\circ}\text{C}$ , 400 cycles, 66.3% retention, 0.5C	[151]
1 M $\text{LiPF}_6$ in PC:DMC + 2 vol% CMDO + 3 vol% EC + 5 vol% FEC	Li/MCMB	$-10\text{ }^{\circ}\text{C}$ , 35 cycles	[152]
1 M $\text{LiPF}_6$ in EC:EMC = 1:2 + 1% $\text{LiDFOB}$	NCM523/graphite	$-20\text{ }^{\circ}\text{C}$ , 93% of its RT capacity, 50 cycles	[131]
1.0 M $\text{LiPF}_6$ in EC:DMC:EMC = 1:1:1 + 1.0% PES	LCO/graphite	$-40\text{ }^{\circ}\text{C}$ , 75% of its RT capacity	[153]
1 M $\text{LiPF}_6$ in EC:EMC:PC = 1:1:1 + 2% FEC	graphite/Li	$-40\text{ }^{\circ}\text{C}$ , 84.5% of its RT capacity, 0.3C	[154]
1 M $\text{LiPF}_6$ in EC:PC:EMC = 1:1:3 + 1% BS	LFP/Li	$-20\text{ }^{\circ}\text{C}$ , 64.8 mAh $\text{g}^{-1}$ , 50 cycles, 1 C	[155]
1 M $\text{LiPF}_6$ in EC:PC:EMC + FEC + VC	NMC/Li	$-40\text{ }^{\circ}\text{C}$ , 85.6 mAh $\text{g}^{-1}$	[156]
1 M $\text{LiPF}_6$ in EC:EMC = 1:2 + 2% $\text{LiPO}_2\text{F}_2$	NCM523/graphite	$-10\text{ }^{\circ}\text{C}$ , 92.7% retention, 0.3C, 100 cycles	[157]
1 M $\text{LiPF}_6$ in EC:PC:EMC:DEC:VC:FEC = 20:5:55:20:2:5 + 1% PDMS-A	LCO/graphite	$-20\text{ }^{\circ}\text{C}$ , 89% retention 0.1C, 50 cycles	[158]
1 M $\text{LiPF}_6$ in EC:DMC = 1:1 + 2% FI	graphite/Li	$-20\text{ }^{\circ}\text{C}$ , 54.1% retention, 0.1C	[159]
1 M $\text{LiPF}_6$ in EC:DMC = 1:1 + $\text{Li-SiB}$ (1 wt%) + PDMS-HT (0.2 wt%)	LCO/graphite	$-20\text{ }^{\circ}\text{C}$ , 84.6% retention, 50 cycles	[160]
1 M $\text{LiPF}_6$ in EC:EMC = 1:2 + PhMS (1 wt%)	NCM523/graphite	$-10\text{ }^{\circ}\text{C}$ , 73.8% retention, 100 cycles	[161]
1 M $\text{LiPF}_6$ in EC:DMC:EMC = 1:1:1 + 2% FEC	graphite/Li	$-20\text{ }^{\circ}\text{C}$ , 55% retention, 10 cycles	[162]
1.3 M $\text{LiPF}_6$ in EC:EMC:DEC = 3:2:5 + 2 wt% AS	graphite/Li	$-30\text{ }^{\circ}\text{C}$ , 0.05C	[126]
<i>Combined method of modification</i>			
	LNO/graphite		[163]

(continued on next page)

Table 3 (continued)

1 M LiBF <sub>4</sub> in PC:EC: EMC = 1:1:3		-30 °C, capacity retention of 86%	
1 M LiBF <sub>4</sub> in EC:PC: EMC = 1:2:7 + 1% FEC	TiO <sub>2</sub> (B)/graphene	-20 °C, 153.4 mAh g <sup>-1</sup> , 95% retention, 2 A g <sup>-1</sup> , 500 cycles	[164]
1 M LiPF <sub>6</sub> in Methyl Acetate:EC:DEC:EMC = 3:1:1:1 + 1% TMSP and 1% PCS	LiNi <sub>0.5</sub> Mn <sub>1.5</sub> O <sub>4</sub> /MCMB	-5 °C, 102 mAh g <sup>-1</sup> , 0.3C, 200 cycles	[165]
1 M LiDFOB in EC:DMC: DMS = 1:1:1 + 4% LiDFP	LNMO/graphite	-20 °C, 72.31% retention, 1 C, 200 cycles	[166]
1 M LiDFOB in IZ:FEC = 10:1 vol.	graphite/Li	-20 °C, 187.5 mAh g <sup>-1</sup> at 0.1C	[167]
1 M LiPF <sub>6</sub> in EC:PC: EMC:DEC = 20:5:55:20 + 2% VC + 2.5% Li2O2 nanosalt	LCO/graphite	-20 °C, -	[168]
1 M LiPF <sub>6</sub> in EC:PC: EMC = 1:1:8 + 0.05 M CsPF <sub>6</sub>	LiNi <sub>0.80</sub> Co <sub>0.15</sub> Al <sub>0.05</sub> O <sub>2</sub> / graphite	-20 °C, 97.5% retention, 0.1C, 100 cycles	[169]
1 M LiPF <sub>6</sub> in EC:PC: EMC:DMC = 1.8:0.3:3.0:3.5 + 1% VC + 0.5% LiBOB	NCM/graphite	-20 °C, 0.74 mAh g <sup>-1</sup> -30 °C, 0.35 mAh, 5 C	[101]
1.28 M LiFSI in FEC: FEMC-D2	LiNi <sub>0.8</sub> Co <sub>0.15</sub> Al <sub>0.05</sub> O <sub>2</sub> /Li	-85 °C, -56% of its RT capacity -20 °C, 150 mAh g <sup>-1</sup> for 450 cycles, 1/3C	[170]
0.75 M LiTFSI in 1,3- dioxan	LCO/LTO	-80 °C, ~60% of its RT capacity, 0.1C	[171]
LiTFSI in PYRIATFSI: EC:PC:EM:FEC	LFP/Li	-30 °C, 73.5 mAh g <sup>-1</sup> , 0.1C	[172]
0.3 M LBF + 0.7 M LPF in DMC:EMC = 3:5 + 16%(V) BA + 10%(V) EC	NCM811/Li	-40 °C, 119.3 mAh g <sup>-1</sup>	[173]
LiPO <sub>2</sub> F <sub>2</sub> /G4/HFE (1/ 1.2/2, by mol) +5% FEC (wt)	NCM523/Li	-60 °C, 70.9 mAh g <sup>-1</sup>	[174]

Abbreviations: MTFP – methyl 3,3,3-trifluoropionate; EMI-BF<sub>4</sub> - 1-ethyl-3-methylimidazolium tetrafluoroborate; NCM523 - LiNi<sub>0.5</sub>Co<sub>0.2</sub>Mn<sub>0.3</sub>O<sub>2</sub>; PFPF - 2,3,4,5,6 - pentafluorophenyl methanesulfonate; TFENH - 2,2,2-Trifluoroethyl N-caproate; D2 - (tetrafluoro-1-(2,2,2-trifluoroethoxy)ethane; FEMC - methyl (2,2,2-trifluoroethyl) carbonate; BA - butyl acrylate; CMDO - 4-Chloromethyl-1,3,2-dioxathiolane-2-oxide; MCMB - mesocarbon microbeads; BS - 1,4-butyl sultone; PYRIATFSI - N-methyl-N-allylpyrrolidinium bis(trifluoromethanesulfonyl)imide; EB - ethyl butyrate; PDMS-A - poly [dimethylsiloxane-co-siloxane-g-acrylate]; FI - fluorosulfonyl isocyanate; PDMS-HT - Hydroxyl-terminated poly(dimethylsiloxane); PhMS - Phenyl methanesulfonate; AS - allyl sulfide; IZ - Isoxazole; RT – room-temperature.

to improve the mobility of Li<sup>+</sup> at low operating temperatures. Since the commonly used electrolyte solvent, EC has a high melting point (36.4 °C) and high viscosity ([Y] = 1.90 cP at 40 °C), reducing its content in the electrolyte (i.e., <25%) and optimization of the blend of linear carbonates (DMC, EMC, DEC) have been proposed as a practical approach [175]. However, a decrease in the viscosity of the electrolyte does not fully ensure an increase in ionic conductivity. So, A. J. Ringsby et al. proposed low-temperature cation transport phenomena should be studied collectively, taking into account the effects of ion association, solvent viscosity, and cation transport number [176]. For example, in its study,  $\gamma$ -butyrolactone (GBL) was used as a low viscosity co-solvent to the electrolyte system of LP57 (1 M LiPF<sub>6</sub> in EC:EMC = 3:7). Although GBL reduces the viscosity of the solution, its low dielectric constant leads to an increase in ion pairing, which does not lead to an improvement in bulk ionic conductivity, nor to a noticeable change in the mechanisms of ion transport.

LT liquid electrolytes can also be obtained by inhibiting the crystallization of EC using additional co-solvents, such as PC. Zhang et al. compared two electrolytes of 1 M LiPF<sub>6</sub> in a mixture of solvents (EC:EMC) with and without PC. Adding PC to electrolytes significantly improved the LT performance of LIBs owing to the formation of less resistive SEI film at the electrolyte-electrode interface [177]. Although the decomposition products of PC during the SEI formation increase the viscosity and deteriorate the ionic conductivity of the electrolyte at low temperatures, authors claim that the properties of the formed SEI film are more detrimental in improving the LT performance of LIBs. The same phenomenon was observed by Kafle et al. after testing 20 combinations of solvent compositions on graphite/NCM111 LIBs: the results showed that the LT performance depended more on the SEI quality than the conductivity of the solvent [153]. On the other hand, electrolyte compositions in which cyclic carbonates (EC, PC) account for less than 25% of the total solvent and solvent compositions with a higher percentage of short-chain linear carbonates (DMC, EMC) improved LT performance. The authors concluded that the LT performance of LIBs could be improved by designing the composition of the most commonly used solvents without commercially unavailable additives. In addition, it has been shown that ternary and quaternary solvent mixtures are better than conventional binary mixtures in producing electrolytes with desirable electrode film characteristics, low melting points, and high conductivity at low temperatures [178].

PC alone is believed to be incompatible with graphite anode as it fails to form uniform passivation layer. Adding cosolvent capable to form ion-solvent-coordinated structure, such as DEC, was found to solve this issue, realizing the reversible lithiation/delithiation of the graphite anode. As a result, in comparison to conventionally used EC-based cells, the pouch cells with the PC-based electrolyte exhibited better LT performance [179].

Using non-carbonate organic esters as co-solvents in electrolytes is another approach to developing electrolytes for LT operation. Properties of certain esters (Fig. 6), such as low viscosity, low melting point, high dielectric constant, and good compatibility with carbon anodes and mixed metal cathodes, can improve LT characteristics of LIBs [143,145]. Methyl formate (MF), methyl acetate (MA), ethyl acetate (EA), ethyl propionate (EP), ethyl butyrate (EB), and methyl butyrate (MB) are commonly studied ester co-solvents used as electrolyte components [146,147,180]. Comparison of MA, EA, EP, and EB as co-solvents has shown that high molecular weight esters generally form more suitable SEIs that are less resistive but more protective, while low molecular weight esters have an ongoing reaction of the electrolyte with the anode and thus a constant build-up of the interface impedance during storage/cycling. Since the improvement in conductivity decreases with increasing chain length or molecular weight, the authors re-confirmed that high ionic conductivity at low temperatures is necessary but insufficient since the ability of esters to form favorable SEI surface films on the carbon electrode is crucial [145,147]. Thus, a prototype cell containing 1.0 M LiPF<sub>6</sub> in EC:EMC:MP = 20:60:20 vol% electrolyte provided six times more capacity than an entire carbonate mixture and could withstand moderate rate at low temperatures down to -60 °C.

Earlier, Sazhin et al. showed that among the variations of MA, EA, Isoamyl acetate (IAA), Isopropyl acetate (IPA), or EP ethers with linear carbonates (DMC, DEC, or EMC), electrolyte compositions containing EP (EC:DMC:EP and EC:EMC:EP) are most promising at -20 °C [180]. On the other hand, electrolyte containing MA (EC:DMC:MA) showed excellent initial performance, rapidly degrading upon subsequent cycles at low temperatures. Xu et al. later attributed it to the high reactivity between MA and MCMB anode with the catalytic formation of the CH<sub>3</sub>O• radical by the MCMB anode [165]. The cycling stability of LIBs with MA-modified electrolytes could be improved by suppressing the side reactions using species derived from binary functional additives, such as tris(trimethylsilyl) phosphite (TMSP) and 1,3-propanediolcyclic sulfate (PCS). Considering the improved conductivity of the MA-modified electrolyte, the authors also support previous studies on



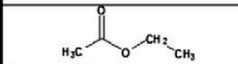
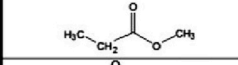
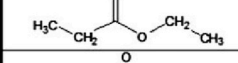
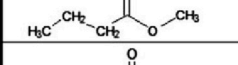
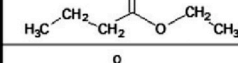
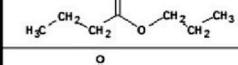
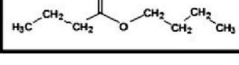
Chemical Structure	Name	m.p.	b.p	Viscosity (25°C)	Density	Dielectric Constant
	Ethyl acetate	-84°C	77°C		0.902	
	Methyl propionate	-87.5°C	79.8°C	0.431 cP	0.915	6.200
	Ethyl propionate	-73°C	99°C		0.888	
	Methyl butyrate	-85.8°C	102.8°C	0.541 cP	0.898	5.48
	Ethyl butyrate	-93°C	120°C	0.639 cP	0.878	5.18
	Propyl butyrate	-95.2°C	143°C		0.873	4.3
	Butyl butyrate	-91.5°C	164°C		0.829	

Fig. 6. Physical properties and chemical structures of candidate ester-based co-solvents investigated in experimental Li-ion cells. (Reproduced with permission from Ref. [147]. Copyright 2010, The Electrochemical Society).

the importance of both high  $\text{Li}^+$  conductivity and the favorable SEI layer for achieving high performance at low temperatures.

Other organic compounds with different functional groups are also successfully studied as co-solvents for electrolyte development at low temperatures. Lu et al. proposed to use about 25 vol% of 2,2,2-Trifluoroethyl N-caproate (TFENH) as a new co-solvent to  $\text{LiPF}_6$  in EC:EMC system [141]. The addition of TFENH decreased the viscosity and increased the ionic conductivity of electrolytes at low temperatures. Furthermore, it decreased the resistance of the SEI film and formed a thin and stable  $\text{CH}_3(\text{CH}_2)_4\text{COOLi}$  film on the anode surface. As a result, the LT performance of graphite-Li and  $\text{LiCoO}_2$ -graphite cells with the modified electrolyte improved significantly.

To solve the LT problems of LIBs, many researchers have focused on the ionic conductivity of the electrolyte. Comparing the  $\text{LiFePO}_4/\text{Li}$  and graphite/Li half-cells, Li et al. proved that ionic conductivity is the main limiting factor for the LT characteristics of the cathode electrolyte [181]. However, for the electrolyte in the anode half-cell, the factors associated with the electrolyte interface are more significant. On the other hand, some researchers opposed the general idea that ionic conductivity is the leading cause of LT battery performance problems [171,182]. The authors stated that the main reason for this problem is the sluggish desolvation at the liquid-solid interface and the reduced migration rate of lithium in the active material. Significantly different characteristics of LIB in electrolytes with similar ionic conductivity once again confirm this point of view. Therefore, a significant increase in the capacity of LIBs at low temperatures can be achieved by reducing the solvent molecule, which binds more strongly to  $\text{Li}^+$  [182]. Xu et al., to enhance the poor temperature performance of LIBs, offered to use an electrolyte such as 1,3-dioxolane-based (DIOX-based) electrolyte because of its low binding energy between  $\text{Li}^+$  and solvent molecules [171]. The DIOX-based electrolyte on nanoscale lithium titanate electrode showed ~60% of the room-temperature capacity at  $-80^\circ\text{C}$  under 0.1C rate. Another effective way of decreasing the affinity between solvents and  $\text{Li}^+$  in the electrolyte is using fluorinated electrolytes [170].

### 5.2.2. Modification of lithium salt

Lithium salt is an essential part of the electrolyte. It can significantly affect the LT performance of a battery because the solubility and degree of dissociation of the lithium salt affect the ionic conductivity of the electrolyte [173,183].

$\text{LiPF}_6$  is considered the most optimal and practical lithium salt due to

its properties, such as good electrochemical stability, the absence of corrosion of the aluminum collector, and high electrical conductivity. Therefore,  $\text{LiPF}_6$  is widely used in electrolytes of LIBs. Nevertheless, this salt has drawbacks, such as difficulty in preparation, poor thermal stability, too high sensitivity to water, and high ionic mobility. Because of these properties of salt, it is challenging to use without losing its characteristics, leading to a high application cost. In addition, the  $R_{ct}$  of LIBs (containing 1 M  $\text{LiPF}_6$  salt in PC:EC:EMC (1:1:3 (wt.)) increases significantly when the temperature drops below  $-10^\circ\text{C}$ , so a high  $R_{ct}$  of graphite and cathode may be another reason for poor LT performance [184]. To improve the LT characteristics of LIBs, Zhang et al. suggested using  $\text{LiBF}_4$  salt instead of  $\text{LiPF}_6$  in  $\text{Li}^+$  electrolytes [163]. The authors claim that although the ionic conductivity of an electrolyte with  $\text{LiBF}_4$  is lower than that of  $\text{LiPF}_6$ , it reduces  $R_{ct}$  and exhibits better LT performance.

Using lithium salts as an electrolyte additive is another promising approach to improving the LT characteristics of LIBs. Since forming a favorable SEI layer is one of the crucial reasons for improving the LT characteristics of LIBs [145,147], the use of lithium salts as additives to the electrolyte gives practical results [148]. However, many of the studied SEI-layer-forming additives are organic, and the SEI layer mainly consists of polymers formed due to their predominant oxidation or reduction. These compounds are poor ion conductors, and even if they create a favorable SEI layer, on the other hand, they increase the interface impedances [134]. Thus, using inorganic lithium salts as electrolyte additives is a perfectly reasonable solution for the poor temperature performance of LIBs. Yang et al. investigated Lithium difluorophosphate ( $\text{LiPO}_2\text{F}_2$ ) as an additive to  $\text{LiNi}_{0.5}\text{Co}_{0.2}\text{Mn}_{0.3}\text{O}_2/\text{graphite}$  cells at low temperatures and showed a significant improvement in capacity compared to cells without additives [148]. The decomposition of  $\text{LiPO}_2\text{F}_2$  resulted in a lower impedance and higher LiF and  $\text{Li}_2\text{CO}_3$  content in the SEI components, forming conductive and stable SEI film on the graphite. Lei et al. also indicated that adding  $\text{LiPO}_2\text{F}_2$  could improve the LT performance of the NCM523/graphite battery by reducing the interface impedance [157]. In addition, S. Kuang et al. illustrated the contribution of  $\text{LiPO}_2\text{F}_2$  to the cathode-electrolyte interface (CEI) with sufficient LiF and P-O components on the NCM523 cathode surface [174]. The formed CEI successfully prevents transition metal ion dissolution and electrolyte decomposition leading to the improved low temperature performance.

Lithium difluoro (oxalate)borate ( $\text{LiDFOB}$ ) is another well-known

lithium salt used for improving low temperature battery characteristics [185]. However, it is proven that traditional electrolyte with LiDFOB has poor temperature performance [166]. Nevertheless, if this salt is combined with another electrolyte system, low temperature performance is improved. For example, S. Tan et al. used isoxazole as the main electrolyte and tested it at  $-20\text{ }^{\circ}\text{C}$  [167]. An electrochemical study has shown the formation of a stable SEI to protect the graphite anode and enable the lithium graphite cell to be cycled providing approximately 9 times the value delivered by the commercial electrolyte. Another use of the salt is as an additive. For example, Chen et al. reported that LNMO/graphite cell performance significantly improved by adding LiDFOB and dimethyl sulfate (DMS) as a co-solvent at low and high temperatures [166]. While the CEI film formed on the cathode by oxidation and decomposition of LiDFOB causes improved battery performance at high temperatures, the improved LT performance is explained by that DMS has a lower melting point and viscosity, and LiDFOB improves the degree of dissociation of electrolytes, which increases ionic conductivity at low temperatures.

Another solution for LiDFOB salt was mixing with  $\text{LiBF}_4$  in equal proportions (1:1, by molar) - in EC:DEC:DMS (1:2:1, vol.) solvents. The combination of the advantages of different salts in an optimized mixed solvent has resulted in excellent film-forming characteristics and low interface film impedance at low temperatures, especially at  $-40\text{ }^{\circ}\text{C}$  [149].

As another example of such additives, Hamenu et al. synthesized a lithium-modified silica nanosalt ( $\text{Li-SiO}_2$ , coded Li202) of hydrophobic fumed silica (R202 (made after polydimethylsiloxane (PDMS) treatment to create a hydrophobic surface)) as an electrolyte additive to improve LT performance of LIBs [168]. The use of a new synthesized LT additive Li202 nanosalt (2.5 wt%) in a 1.0 M  $\text{LiPF}_6$  electrolyte solution dissolved in EC:PC:EMC:DEC (20:5:55:20 vol%) and 2 wt% VC has resulted in higher ionic conductivity. Adding Li202 provides advantages such as electrochemical stabilization of the electrolyte against oxidation at higher voltages. In addition, the authors claim that because of the PDMS surface groups and additional  $\text{Li}^+$  of the electrolyte containing Li202, a better cycle performance at  $-20\text{ }^{\circ}\text{C}$  is provided compared to other electrolytes.

### 5.2.3. Additives

The use of electrolyte additives to improve the LT performance of LIBs is a promising approach to electrolyte modification. Adding small amount of additives (usually up to 5%) to the electrolyte can stabilize and increase battery life by promoting film formation, protecting the anode or cathode, and ensuring battery safety.

Using ionic liquids as an additive is another approach when modifying new electrolytes for LT battery operation. Wang et al. offered to use a 1% 1-ethyl-3-methylimidazolium tetrafluoroborate (EMI- $\text{BF}_4$ ) as an ionic liquid-type electrolyte additive to form stable SEI on  $\text{LiNi}_{0.5}\text{Co}_{0.2}\text{Mn}_{0.3}\text{O}_2$  (NCM523)/graphite batteries to improve the LT performance [150]. The authors state that by adding EMI- $\text{BF}_4$ , battery capacity retention increases by 11.5% after 150 cycles at  $-10\text{ }^{\circ}\text{C}$ , and the discharge capacity almost doubles at  $-30\text{ }^{\circ}\text{C}$ . Zhang et al. synthesized new N-methyl-N-allylpyrrolidinium bis (trifluoromethanesulfonyl) imide (PYR1ATFSI) ionic liquid electrolyte to improve LT battery performance [172]. Studies of the effect of FEC in LiTFSI/PYR1ATFSI:EC:PC:EMC electrolyte on  $\text{LiFePO}_4/\text{Li}$  coin cells have shown promising results at low temperatures down to  $-60\text{ }^{\circ}\text{C}$  due to a decrease in the freezing point and polarization of the composite electrolyte.

Yang et al. presented 2,3,4,5,6-pentafluorophenyl Methanesulfonate (PFPMs) as a versatile additive capable of forming interfacial films on electrode surfaces in  $\text{LiNi}_{0.5}\text{Co}_{0.2}\text{Mn}_{0.3}\text{O}_2/\text{graphite}$  cells over a wide temperature range [151]. The authors compared discharge capacity retention between cells containing 1.0 wt% PFPMs, 1.0 wt% vinylene carbonate (VC), and cells without additive at different temperatures. Comparison results at a low temperature of  $-20\text{ }^{\circ}\text{C}$  show that the discharge capacity retention of the cell with 1.0 wt% PFPMs maintains

66.3% at 0.5C, and for cells without additives and with VC additive, the retention reaches 55.0% and 62.1%, respectively.

To protect against the destruction or freezing of electrolyte components and improve the capacity retention and performance of LIBs at low temperatures, copolymers based on PDMS can be used as additives, which give electrochemical stability provided by the PDMS main chain and grafted functional groups of acrylate, phenyl and ethylene oxide [158].

Another organic SEI ideal layer formation additive researched by Shi et al. is Fluorosulfonyl isocyanate (FI), which has a high recovery potential (over 2.8 V compared to  $\text{Li}/\text{Li}^+$ ) [159]. With the addition of FI, the resistance of the graphite/electrolyte interface decreases; the SEI layer formed by FI consists of a thick and protective inorganic inner layer that prevents the growth of the outer organic layer. One more candidate for forming an SEI film is phenylmethanesulfonate (PhMS) as an LT electrolyte additive. Analytical results showed that adding PhMS to the NCM523/graphite full cell can reduce the impedance of the NCM523/graphite full cell at low temperatures by forming an SEI film on the surface of the graphite anode [161].

Another new additive to solve LT battery problems has been proposed by Phiri et al. [160]. Since biological organisms adapted to low temperatures have zwitterionic molecules with anti-freezing properties in their body, the use of synthesized Zwitterionic lithium-silica sulfo-betaine silane ( $\text{Li-SiSB}$ ) with hydroxyl-terminated poly (dimethylsiloxane) (PDMS-HT) as LT additives to the electrolyte of LIBs is entirely justified. It ensures anti-freezing properties and improved ionic conductivity, and stable SEI formation.

Sulfur-containing organic compounds (allyl sulfide, allyl disulfide, and propyl sulfide) are also suitable electrolyte additives used to improve the poor performance of LIBs at low temperatures. For example, at  $-30\text{ }^{\circ}\text{C}$ , compared to a conventional electrolyte, an electrolyte with a small amount of allyl sulfide (AS) additive in a  $\text{Li}/\text{graphite}$  cell has a reversible graphite electrode capacity of three times. AS has the properties of forming a pre-formed film due to spontaneous oxidation during the soaking period. After repeated cycles, a carbon-rich sulfur-containing film forms at the surface of the graphite, which aids the charge transfer reaction at the graphite electrode, inhibiting lithium plating [126]. Another study on sulfur supplementation used dimethyl sulfoxide (DMSO), which promotes lithium nucleation and creates a strong SEI layer on the lithium metal electrode in extremely cold environments [133]. As a result, lithium metal batteries with DMSO-added electrolyte can provide a discharge capacity of  $51\text{ mAh g}^{-1}$  at  $40\text{ }^{\circ}\text{C}$  at a current of 0.2C. Moreover, SEI has been shown to be resistant to stripping and lithium metal deposition cycles under cold conditions by a series of electrochemical studies carried out at temperatures up to  $80\text{ }^{\circ}\text{C}$ .

### 5.2.4. Combined method of modification

Since both lithium salt and solvents are vital in the electrolyte composition for the LT characteristics of the battery, the combined modification of both salt and solvents in the electrolyte composition can be a comprehensive solution to the problem of LT electrolytes. The main task of the double modification is to lower the melting temperature and viscosity, raise the constant of solvents, develop lithium salts, and improve the compatibility of the components [186,187].

Later, researchers have focused on modifying the  $\text{LiBF}_4$  salt as a lithium salt in the electrolyte because of its reduced  $R_{ct}$ , which gives good performance at low temperatures [163]. Optimization of  $\text{LiBF}_4$  as electrolyte salt in EC:PC:EMC (1:2:7) solvents designed for  $\text{TiO}_2(\text{B})/\text{graphene}$  anode in LIB at low temperature provided a specific capacity of  $\sim 105\text{ mAh g}^{-1}$  at a current density of  $5\text{ A g}^{-1}$  at  $-20\text{ }^{\circ}\text{C}$ . The excellent performance is attributed to the reduced separation energy of the  $\text{Li}^+$  between solvents and the weak interaction between Li and EMC with an optimized composition according to computational simulations [164]. When  $\text{LiBF}_4$  was used as a modified lithium salt in solvents with the addition of BA and EC, modified solvents, to the base electrolyte, the LT discharge capacity of the battery greatly improved. The  $\text{Li}^+$  diffusion

and transport were improved by changing the CEI film properties [173].

Mandal et al. optimized the system of salts and solvents of the electrolyte of a LIB for operation in the temperature range from  $-40$  to  $+70$  °C [188]. Through careful study of the solubility and freezing characteristics of solvent mixtures, a mixture of EC, DMC, and EMC (15:37:48 wt%) has been proposed. The authors also proposed replacing  $\text{LiPF}_6$  with  $\text{LiTFSI}$  according to its stability, high conductivity in any environment, and safety. At  $-40$  °C, the conductivity of the optimized electrolyte composition, 0.9 M  $\text{LiTFSI}$  in EC:DMC:EMC (15:37:48 wt%), is about  $2.0 \text{ mS cm}^{-1}$ .

A new approach to solving the problem of high melting points of electrolytes can be using non-crystallizing mixtures of solvents and lithium electrolytes. Kasprzyk et al. proved that it is possible to prepare a non-crystallizing electrolyte with  $\text{LiTDI}$  (lithium 4,5-dicyano-2-(trifluoromethyl)imidazolid) or  $\text{LiPF}_6$  salt in a mixture of EC with PEG250 (poly(ethylene glycol) dimethyl ether) [178]. Some of these mixtures show a glass transition below  $-70$  °C and relatively high conductivity ( $0.014 \text{ mS cm}^{-1}$ ) at  $-60$  °C.

Another approach is adding additives to organic ester-based electrolytes to improve LT performance further [189]. Smart et al. designed Methyl Butyrate-based electrolyte solutions (EC (20%) and high MB content (60%)), with and without additives (FEC, lithium oxalate, VC,  $\text{LiBOB}$ ) for LT performance [190]. This approach has shown that modified solvents with additives significantly improve the LT discharge rate capability due to forming a favorable SEI layer.

LT charging of a LIB can cause the problem of lithium plating on the surface instead of being intercalated in the anode. Lithium plating and poor LT performance can be corrected by combined electrolyte modification: addition of additive and solvent modification, respectively. Jones et al., as a result of their research, proposed a new electrolyte composition with the addition of lithium bis (fluorosulfonyl)imide ( $\text{LiFSI}$ ) in 1.0 M  $\text{LiPF}_6$  in EC:EMC:MP (20:20:60 vol%), which can reduce the lithium plating at low temperatures [191]. The authors pointed out that adding 0.10 M  $\text{LiFSI}$  additive did not show lithium plating down to  $-40$  °C, which is a good result for charging the cell at lower temperatures. Another investigation was carried out by Piao et al., who used  $\text{LiNO}_3$  as an additive and tetramethylurea as a multifunctional co-solvent to a conventional electrolyte [187]. This modification contributes to the formation of a robust and highly conductive SEI and suppresses HF generation.

## 6. Summary and conclusion

A wide range of factors influences the LT performance of LIBs. Therefore, a complex modification of the whole battery as a system with an optimized choice of electrode materials and electrolyte additives can allow solving the problem. Research on overcoming the electrolyte LT limitations has concentrated on modifying solvents and lithium salts, adding a small amount of organic compounds, or combining modification methods. The electrolyte optimization for LT applications mainly focuses on improving its intrinsic physical properties, such as freezing point, viscosity, ionic conductivity, and chemical composition and properties for film forming on the surfaces of electrodes. The main approaches to address the limitations of the electrode materials at low temperatures include metal or nonmetal doping, surface coating, and morphology control. These approaches are mainly designed aiming at the following enhancements of the electrode materials.

- to improve the lithium-ionic conductivity by enlarging the lattice space and creating additional room for free movement of  $\text{Li}^+$  or by shortening the lithium-ionic path;
- to increase the electrical conductivity by a highly conductive surface coating layer or decrease the band gap of semiconducting materials;
- to stabilize the SEI and CEI layers and reduce the resistance by coating artificial layers or catalyzing the formation of components with high ionic conductivities and restricting the layers overgrowth;

- to improve electrode-electrolyte contact area and increase the number of electrochemically active sites by designing porous nanostructures of different dimensions (1D, 2D, and 3D).

Even though the performance improvement mechanisms and approaches for low temperature are similar to those at room temperature, additional parameters should be considered in the case of LT applications. For instance, conductivity-enhancing modifications should not compromise the stability and resistance of SEI or CEI at low temperatures and vice versa. Since the performance of all LIB components at low temperatures is interdependent and interconnected, the electrode modifications should be studied in conjunction with the electrolyte modifications.

Based on the published data so far, an ideal composition of LIB for LT applications is going to include.

- an anode composed of a nanostructured composite of graphite with conversion-type compounds of high theoretical capacity, demonstrating increased reversibility of lithiation/delithiation reactions at low temperatures (e.g., Sn-based compounds); further research could focus more on  $\text{LiF}$ -coated  $\text{SnO}_2$  anode, demonstrating excellent electrochemical performances even at extremely low temperatures up to  $-50$  °C;
- a cathode made of high-capacity and high-electrical-conductivity compounds with electrolyte-stable microstructure (e.g., surface-treated NCM with an optimized ratio of transition metals); the promising results of thin and uniform  $\text{LiF}$ -rich layer deposition on the NCM surface could be further studied to understand the CEI formation mechanism at low temperatures;
- an electrolyte composed of lithium salt with low desolvation energy (e.g.,  $\text{LiTFSI}$ ) and a mixture of solvents with a low freezing point, high ionic conductivity, low viscosity (e.g., low-molecular-weight esters, such as EA or MP), and stable thin SEI-forming properties (e.g., FEC or VC). For instance, the effect of 1 M  $\text{LiTFSI}$  in MP:FEC = 9:1 (wt.) on the LT properties of different cathode and anode materials and improvement mechanisms could be further investigated in detail.

On the other hand, the possibility of combining such components into one LT LIB and other novel configurations should be further extensively investigated.

Finally, we would like to conclude by pointing out several research flaws for LT LIBs that deserve greater attention, and tackling them might make LIBs operable at ultra-low temperatures. The most obvious of these is that the advancement of electrolyte systems for LT operation needs to consider both the conductivity of electrolyte systems and the better performance of targeted electrodes, which requires in-depth elaboration and a combination of electrolyte composition and structure and electrode reaction mechanism. Moreover, from this review, it can be noted that the novel electrolyte systems in combination with additives were generally developed and studied only for specific cathodes or anodes alone. Electrolytes, which positively affect both electrodes in a full cell, need to be designed and investigated. Additionally, it is worth mentioning that there is scarce research on the relationship between electrode crystal structure and solid-state ion diffusion at low temperatures. Due to the direct influence of lattice dimensions on ion diffusion, especially at low temperature, it is promising to investigate this relationship thoroughly from a new perspective of capabilities of novel state-of-the-art in-situ and operando techniques and modify the electrode crystal structure on this basis accordingly. More complex structures such as core-shell, gradient, and 3D architectures rather than doping and coating might help in solving the problem of slow diffusion of lithium metal ions. Further, along with electrodes and electrolytes, other battery components such as current collectors, separators, binders, and conductive agents also need to be investigated. Last but not the least, battery testing protocols at low temperatures must not be



overlooked, taking into account the real conditions in practice where the battery, in most cases, is charged at room temperature and only discharged at low temperatures depending on the field of application.

We believe that the collective knowledge currently available and that will be obtained in the coming years in the field of LT LIBs will make it possible to construct a battery operable at ultra-low temperatures allowing us to use our phones and drive our cars outside at  $-30\text{ }^{\circ}\text{C}$ , or even fly across the space.

#### Declaration of competing interest

The authors declare that they have no known competing financial interests or personal relationships that could have appeared to influence the work reported in this paper.

#### Data availability

Data will be made available on request.

#### Acknowledgment

This research was funded by the research grant #51763/IIIQΦ-MIIPOAII PK-19 from the Ministry of Digital Development, Innovations, and Aerospace Industry of the Republic of Kazakhstan.

#### Appendix A. Supplementary data

Supplementary data to this article can be found online at <https://doi.org/10.1016/j.jpowsour.2022.232550>.

#### References

- [1] C. Wei, Y. Zhang, Y. Tian, L. Tan, Y. An, Y. Qian, B. Xi, S. Xiong, J. Feng, Y. Qian, Design of safe, long-cycling and high-energy lithium metal anodes in all working conditions: progress, challenges and perspectives, *Energy Storage Mater.* 38 (2021) 157–189.
- [2] G. Zhang, X. Wei, G. Han, H. Dai, J. Zhu, X. Wang, X. Tang, J. Ye, Lithium plating on the anode for lithium-ion batteries during long-term low temperature cycling, *J. Power Sources* 484 (2021), 229312.
- [3] A. Senyshyn, M.J. Mühlbauer, O. Dolotko, H. Ehrenberg, Low-temperature performance of Li-ion batteries: the behavior of lithiated graphite, *J. Power Sources* 282 (2015) 235–240.
- [4] E.J. Plichta, W.K. Behl, Low-temperature electrolyte for lithium and lithium-ion batteries, *J. Power Sources* 88 (2000) 192–196.
- [5] J. Jaguemont, L. Boulon, Y. Dubé, A comprehensive review of lithium-ion batteries used in hybrid and electric vehicles at cold temperatures, *Appl. Energy* 164 (2016) 99–114.
- [6] Z. Lei, Y. Zhang, X. Lei, Improving temperature uniformity of a lithium-ion battery by intermittent heating method in cold climate, *Int. J. Heat Mass Tran.* 121 (2018) 275–281.
- [7] W. Zhao, Y. Ji, Z. Zhang, M. Lin, Z. Wu, X. Zheng, Q. Li, Y. Yang, Recent advances in the research of functional electrolyte additives for lithium-ion batteries, *Curr. Opin. Electrochem.* 6 (2017) 84–91.
- [8] T. van Ree, Electrolyte additives for improved lithium-ion battery performance and overcharge protection, *Curr. Opin. Electrochem.* 21 (2020) 22–30.
- [9] N. Xu, J. Shi, G. Liu, X. Yang, J. Zheng, Z. Zhang, Y. Yang, Research progress of fluorine-containing electrolyte additives for lithium ion batteries, *J. Power Sources Adv.* 7 (2021), 100043.
- [10] G. Zhu, K. Wen, W. Lv, X. Zhou, Y. Liang, F. Yang, Z. Chen, M. Zou, J. Li, Y. Zhang, W. He, Materials insights into low-temperature performances of lithium-ion batteries, *J. Power Sources* 300 (2015) 29–40.
- [11] A. Gupta, A. Manthiram, Designing advanced lithium-based batteries for low-temperature conditions, *Adv. Energy Mater.* 10 (2020) 1–14.
- [12] J. Zhang, J. Zhang, T. Liu, H. Wu, S. Tian, L. Zhou, B. Zhang, G. Cui, Toward low-temperature lithium batteries: advances and prospects of unconventional electrolytes, *Adv. Energy Sustain. Res.* (2021), 2100039.
- [13] Y. Na, X. Sun, A. Fan, S. Cai, C. Zheng, Methods for enhancing the capacity of electrode materials in low-temperature lithium-ion batteries, *Chin. Chem. Lett.* 32 (2021) 973–982.
- [14] F. Meng, X. Xiong, L. Tan, B. Yuan, R. Hu, Strategies for improving electrochemical reaction kinetics of cathode materials for subzero-temperature Li-ion batteries: a review, *Energy Storage Mater.* 44 (2022) 390–407.
- [15] G.A. Collins, H. Geaney, K.M. Ryan, Alternative anodes for low temperature lithium-ion batteries, *J. Mater. Chem.* 9 (2021) 14172–14213.
- [16] D. Hubble, D.E. Brown, Y. Zhao, C. Fang, J. Lau, B.D. McCloskey, G. Liu, Liquid electrolyte development for low-temperature lithium-ion batteries, *Energy Environ. Sci.* 15 (2022) 550–578.
- [17] D. Zhang, C. Tan, T. Ou, S. Zhang, L. Li, X. Ji, Constructing advanced electrode materials for low-temperature lithium-ion batteries: a review, *Energy Rep.* 8 (2022) 4525–4534.
- [18] W. Lin, M. Zhu, Y. Fan, H. Wang, G. Tao, M. Ding, N. Liu, H. Yang, J. Wu, J. Fang, Y. Tang, Low temperature lithium-ion batteries electrolytes: rational design, advancements, and future perspectives, *J. Alloys Compd.* 905 (2022), 164163.
- [19] X. Pang, B. An, S. Zheng, B. Wang, Cathode materials of metal-ion batteries for low-temperature applications, *J. Alloys Compd.* 912 (2022).
- [20] J. Hou, M. Yang, D. Wang, J. Zhang, Fundamentals and challenges of lithium ion batteries at temperatures between  $-40$  and  $60\text{ }^{\circ}\text{C}$ , *Adv. Energy Mater.* 10 (2020) 1–23.
- [21] N. Piao, X. Gao, H. Yang, Z. Guo, G. Hu, H.M. Cheng, F. Li, Challenges and development of lithium-ion batteries for low temperature environments, *ETransportation* 11 (2022), 100145.
- [22] M.-T.F. Rodrigues, G. Babu, H. Gullapalli, K. Kalaga, F.N. Sayed, K. Kato, J. Joyner, P.M. Ajayan, A materials perspective on Li-ion batteries at extreme temperatures, *Nat. Energy* 2 (2017) 1–14.
- [23] N. Zhang, T. Deng, S. Zhang, C. Wang, L. Chen, C. Wang, X. Fan, Critical review on low-temperature Li-Ion/Metal batteries, *Adv. Mater.* 34 (2022), 2107899.
- [24] B.E. Worku, S. Zheng, B. Wang, Review of low-temperature lithium-ion battery progress: new battery system design imperative, *Int. J. Energy Res.* (2022) 1–18.
- [25] T.L. Kulova, A.M. Skundin, A critical review of electrode materials and electrolytes for low-temperature lithium-ion batteries, *Int. J. Electrochem. Sci.* 15 (2020) 8638–8661.
- [26] A. Hu, F. Li, W. Chen, T. Lei, Y. Li, Y. Fan, M. He, F. Wang, M. Zhou, Y. Hu, Y. Yan, B. Chen, J. Zhu, J. Long, X. Wang, J. Xiong, Ion transport kinetics in low-temperature lithium metal batteries, *Adv. Energy Mater.* 12 (2022), 2202432.
- [27] X. Dong, Y.-G. Wang, Y. Xia, Promoting rechargeable batteries operated at low temperature, *Acc. Chem. Res.* 54 (2021) 3883–3894.
- [28] J. Xu, X. Wang, N. Yuan, B. Hu, J. Ding, S. Ge, Graphite-based lithium ion battery with ultrafast charging and discharging and excellent low temperature performance, *J. Power Sources* 430 (2019) 74–79.
- [29] J. Wu, T. Li, H. Zhang, Y. Lei, G. Zhou, Research on modeling and SOC estimation of lithium iron phosphate battery at low temperature, *Energy Proc.* 152 (2018) 556–561.
- [30] L. Wang, A. Menakath, F. Han, Y. Wang, P.Y. Zavalij, K.J. Gaskell, O. Borodin, D. Iuga, S.P. Brown, C. Wang, K. Xu, B.W. Eichhorn, Identifying the components of the solid–electrolyte interphase in Li-ion batteries, *Nat. Chem.* 11 (2019) 789–796.
- [31] A.C. Thenuwara, P.P. Shetty, N. Kondekar, S.E. Sandoval, K. Cavallaro, R. May, C. T. Yang, L.E. Marbella, Y. Qi, M.T. McDowell, Efficient low-temperature cycling of lithium metal anodes by tailoring the solid-electrolyte interphase, *ACS Energy Lett.* 5 (2020) 2411–2420.
- [32] G. Nagasubramanian, D.H. Doughty, 18650 Li-ion cells with reference electrode and in situ characterization of electrodes, *J. Power Sources* 150 (2005) 182–186.
- [33] D. Hu, G. Chen, J. Tian, N. Li, L. Chen, Y. Su, T. Song, Y. Lu, D. Cao, S. Chen, F. Wu, Unrevealing the effects of low temperature on cycling life of 21700-type cylindrical Li-ion batteries, *J. Energy Chem.* 60 (2021) 104–110.
- [34] J. Li, S. Li, Y. Zhang, Y. Yang, S. Russi, G. Qian, L. Mu, S.J. Lee, Z. Yang, J.S. Lee, P. Pianetta, J. Qiu, D. Ratner, P. Cloetens, K. Zhao, F. Lin, Y. Liu, Multiphase, multiscale chemomechanics at extreme low temperatures: battery electrodes for operation in a wide temperature range, *Adv. Energy Mater.* 2102122 (2021) 1–9.
- [35] J.Y. Eom, L. Cao, Effect of anode binders on low-temperature performance of automotive lithium-ion batteries, *J. Power Sources* 441 (2019), 227178.
- [36] Y. Guo, D. Li, R. Xiong, H. Li, Investigation of the temperature-dependent behaviours of Li metal anode, *Chem. Commun.* 55 (2019) 9773–9776.
- [37] M. Petzl, M. Kasper, M.A. Danzer, Lithium plating in a commercial lithium-ion battery - a low-temperature aging study, *J. Power Sources* 275 (2015) 799–807.
- [38] G. Park, N. Gunawardhana, H. Nakamura, Y.S. Lee, M. Yoshio, The study of electrochemical properties and lithium deposition of graphite at low temperature, *J. Power Sources* 199 (2012) 293–299.
- [39] F. Nobili, M. Mancini, S. Dsoke, R. Tossici, R. Marassi, Low-temperature behavior of graphite-tin composite anodes for Li-ion batteries, *J. Power Sources* 195 (2010) 7090–7097.
- [40] Q. Meng, F. Chen, Q. Hao, N. Li, X. Sun, Nb-doped  $\text{Li}_4\text{Ti}_5\text{O}_{12}\text{-TiO}_2$  hierarchical microspheres as anode materials for high-performance Li-ion batteries at low temperature, *J. Alloys Compd.* 885 (2021).
- [41] F. Nobili, S. Dsoke, T. Mecozzi, R. Marassi, Metal-oxidized graphite composite electrodes for lithium-ion batteries, *Electrochim. Acta* 51 (2005) 536–544.
- [42] Y. Yan, L. Ben, Y. Zhan, X. Huang, Nano-Sn embedded in expanded graphite as anode for lithium ion batteries with improved low temperature electrochemical performance, *Electrochim. Acta* 187 (2016) 186–192.
- [43] R. Akolkar, Modeling dendrite growth during lithium electrodeposition at sub-ambient temperature, *J. Power Sources* 246 (2014) 84–89.
- [44] N. Zhao, F. Zhang, F. Zhan, D. Yi, Y. Yang, W. Cui, X. Wang,  $\text{Fe}^{3+}$ -stabilized  $\text{Ti}_3\text{C}_2\text{TxMXene}$  enables ultrastable Li-ion storage at low temperature, *J. Mater. Sci. Technol.* 67 (2021) 156–164.
- [45] Z. Bai, X. Lv, D.H. Liu, D. Dai, J. Gu, L. Yang, Z. Chen, Two-Dimensional NiO@C-N nanosheets composite as a superior low-temperature anode material for advanced lithium-/sodium-ion batteries, *Chemelectrochem* 7 (2020) 3616–3622.
- [46] M. Marinaro, M. Pfanzelt, P. Kubiak, R. Marassi, M. Wohlfahrt-Mehrens, Low temperature behaviour of  $\text{TiO}_2$  rutile as negative electrode material for lithium-ion batteries, *J. Power Sources* 196 (2011) 9825–9829.

- [47] C. Stetson, Y. Yin, C.S. Jiang, S.C. Decaluwe, M. Al-Jassim, N.R. Neale, C. Ban, A. Burrell, Temperature-dependent solubility of solid electrolyte interphase on silicon electrodes, *ACS Energy Lett.* 4 (2019) 2770–2775.
- [48] H. Dong, J. Wang, P. Wang, H. Ding, R. Song, N.S. Zhang, D.N. Zhao, L.J. Zhang, S.Y. Li, Effect of temperature on formation and evolution of solid electrolyte interphase on Si@Graphite@C anodes, *J. Energy Chem.* 64 (2022) 190–200.
- [49] S.H. Beheshti, M. Javanbakht, H. Omidvar, M.S. Hosen, A. Hubin, J. Van Mierlo, M. Bercibar, Development, retainment, and assessment of the graphite-electrolyte interphase in Li-ion batteries regarding the functionality of SEI-forming additives, *iScience* 25 (2022).
- [50] E. Markevich, G. Salitra, D. Aurbach, Low temperature performance of amorphous monolithic silicon anodes: comparative study of silicon and graphite electrodes, *J. Electrochem. Soc.* 163 (2016) A2407–A2412.
- [51] S. He, S. Huang, S. Wang, I. Mizota, X. Liu, X. Hou, Considering critical factors of silicon/graphite anode materials for practical high-energy lithium-ion battery applications, *Energy Fuel.* 35 (2021) 944–964.
- [52] N.M. Johnson, Z. Yang, M. Kim, D.J. Yoo, Q. Liu, Z. Zhang, Enabling silicon anodes with novel isosorbide-based electrolytes, *ACS Energy Lett.* 7 (2022) 897–905.
- [53] S. Chae, W.J. Kwak, K.S. Han, S. Li, M.H. Engelhard, J. Hu, C. Wang, X. Li, J. G. Zhang, Rational design of electrolytes for long-term cycling of Si anodes over a wide temperature range, *ACS Energy Lett.* 6 (2021) 387–394.
- [54] P. Li, H. Kim, S.T. Myung, Y.K. Sun, Diverting exploration of silicon anode into practical way: a review focused on silicon-graphite composite for lithium ion batteries, *Energy Storage Mater.* 35 (2021) 550–576.
- [55] L. Tan, R. Hu, H. Zhang, X. Lan, J. Liu, H. Wang, B. Yuan, M. Zhu, Subzero temperature promotes stable lithium storage in SnO<sub>2</sub>, *Energy Storage Mater.* 36 (2021) 242–250.
- [56] M. Mancini, F. Nobili, S. Dsoke, F. D'Amico, R. Tossici, F. Croce, R. Marassi, Lithium intercalation and interfacial kinetics of composite anodes formed by oxidized graphite and copper, *J. Power Sources* 190 (2009) 141–148.
- [57] R. Raccichini, A. Varzi, V.S.K. Chakravadhanula, C. Kübel, A. Balducci, S. Passerini, Enhanced low-temperature lithium storage performance of multilayer graphene made through an improved ionic liquid-assisted synthesis, *J. Power Sources* 281 (2015) 318–325.
- [58] M.J. Lee, K. Lee, J. Lim, M. Li, S. Noda, S.J. Kwon, B. DeMattia, B. Lee, S.W. Lee, Outstanding low-temperature performance of structure-controlled graphene anode based on surface-controlled charge storage mechanism, *Adv. Funct. Mater.* 31 (2021) 1–12.
- [59] Z. Gao, X. Zhang, H. Hu, D. Guo, H. Zhao, H. Yu, Influencing factors of low- and high-temperature behavior of Co-doped Zn<sub>2</sub>SnO<sub>4</sub>-graphene-carbon nanocomposite as anode material for lithium-ion batteries, *J. Electroanal. Chem.* 791 (2017) 56–63.
- [60] J.L. Allen, T.R. Jow, J. Wolfenstine, Low temperature performance of nonphase Li<sub>4</sub>Ti<sub>5</sub>O<sub>12</sub>, *J. Power Sources* 159 (2006) 1340–1345.
- [61] T. Yuan, X. Yu, R. Cai, Y. Zhou, Z. Shao, Synthesis of pristine and carbon-coated Li<sub>4</sub>Ti<sub>5</sub>O<sub>12</sub> and their low-temperature electrochemical performance, *J. Power Sources* 195 (2010) 4997–5004.
- [62] B. Hu, X. Zhou, J. Xu, X. Wang, N. Yuan, S. Ge, J. Ding, Excellent rate and low temperature performance of lithium-ion batteries based on binder-free Li<sub>4</sub>Ti<sub>5</sub>O<sub>12</sub> electrode, *ChemElectrochem* 7 (2020) 716–722.
- [63] Z. Pu, Q. Lan, Y. Li, S. Liu, D. Yu, X.J. Lv, Preparation of W-doped hierarchical porous Li<sub>4</sub>Ti<sub>5</sub>O<sub>12</sub>/brookite nanocomposites for high rate lithium ion batteries at –20 °C, *J. Power Sources* 437 (2019), 226890.
- [64] J. Li, Y. Li, Q. Lan, Z. Yang, X.J. Lv, Multiple phase N-doped TiO<sub>2</sub> nanotubes/TiN/graphene nanocomposites for high rate lithium ion batteries at low temperature, *J. Power Sources* 423 (2019) 166–173.
- [65] X.H. Ma, X. Cao, Y.Y. Ye, F. Qiao, M.F. Qian, Y.Y. Wei, Y.D. Wu, Z.F. Zi, J.M. Dai, Study on low-temperature performances of Nb<sub>16</sub>W<sub>5</sub>O<sub>55</sub> anode for lithium-ion batteries, *Solid State Ionics* 353 (2020), 115376.
- [66] C. Liang, Y. Tao, N. Yang, D. Huang, S. Li, K. Han, Y. Luo, H. Chen, L. Mai, Bubble-templated synthesis of Fe<sub>2</sub>(MoO<sub>4</sub>)<sub>3</sub> hollow hierarchical microsphere with superior low-temperature behavior and high areal capacity for lithium ion batteries, *Electrochim. Acta* 311 (2019) 192–200.
- [67] J. Li, W. Wen, G. Xu, M. Zou, Z. Huang, L. Guan, Fe-added Fe<sub>3</sub>C carbon nanofibers as anode for Li ion batteries with excellent low-temperature performance, *Electrochim. Acta* 153 (2015) 300–305.
- [68] I.M. Gavrillin, Y.O. Kudryashova, A.A. Kuz'mina, T.L. Kulova, A.M. Skundin, V. V. Emets, R.L. Volkov, A.A. Dronov, N.I. Borgardt, S.A. Gavrillov, High-rate and low-temperature performance of germanium nanowires anode for lithium-ion batteries, *J. Electroanal. Chem.* 888 (2021), 115209.
- [69] G.A. Collins, K. McNamara, S. Kilian, H. Geaney, K.M. Ryan, Alloying germanium nanowire anodes dramatically outperform graphite anodes in full-cell chemistries over a wide temperature range, *ACS Appl. Energy Mater.* 4 (2021) 1793–1804.
- [70] A. Varzi, L. Mattarozzi, S. Cattarin, P. Guerriero, S. Passerini, 3D porous Cu–Zn alloys as alternative anode materials for Li-ion batteries with superior low T performance, *Adv. Energy Mater.* 8 (2018) 1–11.
- [71] W. Ma, Y. Wang, Y. Yang, X. Wang, Z. Yuan, X. Liu, Y. Ding, Temperature-dependent Li storage performance in nanoporous Cu–Ge–Al alloy, *ACS Appl. Mater. Interfaces* 11 (2019) 9073–9082.
- [72] M. Zou, J. Li, W. Wen, L. Chen, L. Guan, H. Lai, Z. Huang, Silver-incorporated composites of Fe<sub>2</sub>O<sub>3</sub> carbon nanofibers as anodes for high-performance lithium batteries, *J. Power Sources* 270 (2014) 468–474.
- [73] Q. Chen, W. Zhong, J. Zhang, C. Gao, W. Liu, G. Li, M. Ren, Fe<sub>3</sub>O<sub>4</sub> nanorods in N-doped carbon matrix with pseudo-capacitive behaviors as an excellent anode for subzero lithium-ion batteries, *J. Alloys Compd.* 772 (2019) 557–564.
- [74] L. Tan, X. Lan, R. Hu, J. Liu, B. Yuan, M. Zhu, Stable lithium storage at subzero temperatures for high-capacity Co<sub>3</sub>O<sub>4</sub>@graphene composite anodes, *ChemNanoMat* 7 (2021) 61–70.
- [75] L. Tan, X. Lan, J. Chen, H. Zhang, R. Hu, M. Zhu, LiF-Induced stable solid electrolyte interphase for a wide temperature SnO<sub>2</sub>-based anode extensible to –50 °C, *Adv. Energy Mater.* 2101855 (2021), 2101855.
- [76] H. Fan, F. Bahmani, Y.V. Kaneti, Y. Guo, A.A. Alothman, X. Wu, Y. Yamauchi, W. Li, J. Zhang, Pseudocapacitive lithium storage of cauliflower-like CoFe<sub>2</sub>O<sub>4</sub> for low-temperature battery operation, *Chem. Eur J.* 26 (2020) 13652–13658.
- [77] L. Yu, S.-X. Zhao, Y. Yuan, G.-D. Wei, Improving the room/low-temperature performance of VS<sub>4</sub> anode by regulating the sulfur vacancy and microstructure, *Electrochim. Acta* 384 (2021), 138351.
- [78] H.H. Fan, H.H. Li, J.Z. Guo, Y.P. Zheng, K.C. Huang, C.Y. Fan, H.Z. Sun, X.F. Li, X. L. Wu, J.P. Zhang, Target construction of ultrathin graphitic carbon encapsulated FeS hierarchical microspheres featuring superior low-temperature lithium/sodium storage properties, *J. Mater. Chem.* 6 (2018) 7997–8005.
- [79] F. Lu, J. Liu, J. Xia, Y. Yang, X. Wang, Engineering C–N moieties in branched nitrogen-doped graphite tubular foam toward stable Li+–Storage at low temperature, *Ind. Eng. Chem. Res.* 59 (2020) 5858–5864.
- [80] Y. Xue, H. Li, Y. Zhang, K. Zhuo, G. Bai, Construction of rich conductive pathways from bottom to top: a highly efficient charge-transfer system used in durable Li/Na-ion batteries at –20 °C, *Chem. Eur J.* 26 (2020) 13274–13281.
- [81] Z. Syum, T. Billo, A. Sabbah, B. Venugopal, S.Y. Yu, F.Y. Fu, H.L. Wu, L.C. Chen, K.H. Chen, Copper zinc tin sulfide anode materials for lithium-ion batteries at low temperature, *ACS Sustain. Chem. Eng.* 9 (2021) 8970–8979.
- [82] H.H. Fan, H.H. Li, Z.W. Wang, W.L. Li, J.Z. Guo, C.Y. Fan, H.Z. Sun, X.L. Wu, J. P. Zhang, Tailoring coral-like Fe<sub>7</sub>Se<sub>8</sub>@C for superior low-temperature Li/Na-ion half/full batteries: synthesis, structure, and DFT studies, *ACS Appl. Mater. Interfaces* 11 (2019) 47886–47893.
- [83] M. Uhlemann, M. Madian, R. Leones, S. Oswald, S. Maletti, A. Eychmüller, D. Mikhailova, In-depth study of Li<sub>4</sub>Ti<sub>5</sub>O<sub>12</sub> performing beyond conventional operating conditions, *ACS Appl. Mater. Interfaces* 12 (2020) 37227–37238.
- [84] A. Nurpeissova, A. Adi, A. Aishova, A. Mukanova, S.S. Kim, Z. Bakenov, Synergistic effect of 3D current collector structure and Ni inactive matrix on the electrochemical performances of Sn-based anodes for lithium-ion batteries, *Mater. Today Energy* 16 (2020), 100397.
- [85] P. Nithyadharseni, M.V. Reddy, B. Nalini, M. Kalpana, B.V.R. Chowdari, Sn-Based intermetallic alloy anode materials for the application of lithium ion batteries, *Electrochim. Acta* 161 (2015) 261–268.
- [86] X. Liu, Y. Wang, Y. Yang, W. Lv, G. Lian, D. Golberg, X. Wang, X. Zhao, Y. Ding, A MoS<sub>2</sub>/Carbon hybrid anode for high-performance Li-ion batteries at low temperature, *Nano Energy* 70 (2020), 104550.
- [87] N. Issatayev, A. Nurpeissova, G. Kalimuldina, Z. Bakenov, Three-dimensional foam-type current collectors for rechargeable batteries: a short review, *J. Power Sources Adv.* 10 (2021), 100065.
- [88] M. Marinaro, M. Mancini, F. Nobili, R. Tossici, L. Damen, R. Marassi, A newly designed Cu/Super-P composite for the improvement of low-temperature performances of graphite anodes for lithium-ion batteries, *J. Power Sources* 222 (2013) 66–71.
- [89] G. Nagasubramanian, Electrical characteristics of 18650 Li-ion cells at low temperatures, *J. Appl. Electrochem.* 31 (2001) 99–104.
- [90] H. Wang, X. Li, F. Li, X. Liu, S. Yang, J. Ma, Formation and modification of cathode electrolyte interphase: a mini review, *Electrochem. Commun.* 122 (2021), 106870.
- [91] D. Becker, G. Cherkashinin, R. Hausbrand, W. Jaegermann, XPS study of diethyl carbonate adsorption on LiCoO<sub>2</sub> thin films, *Solid State Ionics* 230 (2013) 83–85.
- [92] D. Becker, G. Cherkashinin, R. Hausbrand, W. Jaegermann, Adsorption of diethyl carbonate on LiCoO<sub>2</sub> thin films: formation of the electrochemical interface, *J. Phys. Chem. C* 118 (2014) 962–967.
- [93] J. Wandt, A. Freiberg, R. Thomas, Y. Gorlin, A. Siebel, R. Jung, H.A. Gasteiger, M. Tromp, Transition metal dissolution and deposition in Li-ion batteries investigated by operando X-ray absorption spectroscopy, *J. Mater. Chem.* 4 (2016) 18300–18305.
- [94] L. Yang, M. Takahashi, B. Wang, A study on capacity fading of lithium-ion battery with manganese spinel positive electrolyte during cycling, *Electrochim. Acta* 51 (2006) 3228–3234.
- [95] D. Ouyang, Y. He, J. Weng, J. Liu, M. Chen, J. Wang, Influence of low temperature conditions on lithium-ion batteries and the application of an insulation material, *RSC Adv.* 9 (2019) 9053–9066.
- [96] Y. Li, K. Qian, Y.B. He, Y.V. Kaneti, D. Liu, D. Luo, H. Li, B. Li, F. Kang, Study on the reversible capacity loss of layered oxide cathode during low-temperature operation, *J. Power Sources* 342 (2017) 24–30.
- [97] W. Wu, W. Wu, X. Qiu, S. Wang, Low-temperature reversible capacity loss and aging mechanism in lithium-ion batteries for different discharge profiles, *Int. J. Energy Res.* 43 (2019) 243–253.
- [98] Y. Wang, Z. Chu, X. Feng, X. Han, L. Lu, J. Li, M. Ouyang, Overcharge durability of Li<sub>4</sub>Ti<sub>5</sub>O<sub>12</sub> based lithium-ion batteries at low temperature, *J. Energy Storage* 19 (2018) 302–310.
- [99] Y. Wu, P. Keil, S.F. Schuster, A. Jossen, Impact of temperature and discharge rate on the aging of a LiCoO<sub>2</sub>/LiNi<sub>0.8</sub>Co<sub>0.15</sub>Al<sub>0.05</sub>O<sub>2</sub> lithium-ion pouch cell, *J. Electrochem. Soc.* 164 (2017) A1438–A1445.
- [100] X.L. Wu, Y.G. Guo, J. Su, J.W. Xiong, Y.L. Zhang, L.J. Wan, Carbon-nanotube-decorated nano-LiFePO<sub>4</sub> @c cathode material with superior high-rate and low-temperature performances for lithium-ion batteries, *Adv. Energy Mater.* 3 (2013) 1155–1160.

- [101] H. Zhang, Y. Xu, C. Zhao, X. Yang, Q. Jiang, Effects of carbon coating and metal ions doping on low temperature electrochemical properties of LiFePO<sub>4</sub> cathode material, *Electrochim. Acta* 83 (2012) 341–347.
- [102] C. Xu, J. Li, X. Feng, J. Zhao, C. Tang, B. Ji, J. Hu, C. Cao, Y. Zhu, F.K. Butt, The improved performance of spinel LiMn<sub>2</sub>O<sub>4</sub> cathode with micro-nanostructured sphere-interconnected-tube morphology and surface orientation at extreme conditions for lithium-ion batteries, *Electrochim. Acta* 358 (2020).
- [103] Z. Chen, J.R. Dahn, Reducing carbon in LiFePO<sub>4</sub>/C composite electrodes to maximize specific energy, volumetric energy, and tap density, *J. Electrochem. Soc.* 149 (2002), A1184.
- [104] N. Tolganbek, Y. Yerkinbekova, S. Kalybekkyzy, Z. Bakenov, A. Mentbayeva, Current state of high voltage olivine structured LiMPO<sub>4</sub> cathode materials for energy storage applications: a review, *J. Alloys Compd.* 882 (2021), 160774.
- [105] X. Yang, Y. Xu, H. Zhang, Y. Huang, Q. Jiang, C. Zhao, Enhanced high rate and low-temperature performances of mesoporous LiFePO<sub>4</sub>/Ketjen Black nanocomposite cathode material, *Electrochim. Acta* 114 (2013) 259–264.
- [106] X. Cui, K. Tuo, Y. Xie, C. Li, D. Zhao, L. Yang, X. Fu, S. Li, Investigation on electrochemical performance at the low temperature of LFP/C-P composite based on phosphorus doping carbon network, *Ionics* 26 (2020) 3795–3808.
- [107] N. Zhao, X. Zhi, L. Wang, Y. Liu, G. Liang, Effect of microstructure on low temperature electrochemical properties of LiFePO<sub>4</sub>/C cathode material, *J. Alloys Compd.* 645 (2015) 301–308.
- [108] Y. Gao, K. Xiong, H. Xu, B. Zhu, Enhanced high-rate and low-temperature electrochemical properties of LiFePO<sub>4</sub>/polypyrrole cathode materials for lithium-ion batteries, *Int. J. Electrochem. Sci.* 14 (2019) 3408–3417.
- [109] C.C. Yang, J.H. Jang, J.R. Jiang, Study of electrochemical performances of lithium titanium oxide-coated LiFePO<sub>4</sub>/C cathode composite at low and high temperatures, *Appl. Energy* 162 (2016) 1419–1427.
- [110] Y. ju Lv, B. Huang, J. xu Tan, S. quan Jiang, S. fen Zhang, Y. xuan Wen, Enhanced low temperature electrochemical performances of LiFePO<sub>4</sub>/C by V<sup>3+</sup> and F<sup>-</sup> co-doping, *Mater. Lett.* 229 (2018) 349–352.
- [111] Z. Li, X. Ren, Y. Zheng, W. Tian, L. An, J. Sun, R. Ding, L. Wen, G. Liang, Effect of Ti doping on LiFePO<sub>4</sub>/C cathode material with enhanced low-temperature electrochemical performance, *Ionics* 26 (2020) 1599–1609.
- [112] Y.G. Cho, M. Li, J. Holoubek, W. Li, Y. Yin, Y.S. Meng, Z. Chen, Enabling the low-temperature cycling of NMC||Graphite pouch cells with an ester-based electrolyte, *ACS Energy Lett.* 6 (2021) 2016–2023.
- [113] X. Shanguan, G. Xu, Z. Cui, Q. Wang, X. Du, K. Chen, S. Huang, G. Jia, F. Li, X. Wang, D. Lu, S. Dong, G. Cui, Additive-Assisted metal dual-salt electrolyte addresses wide temperature operation of lithium–nickel batteries, *Small* 15 (2019) 1–8.
- [114] S. Cui, Y. Wei, T. Liu, W. Deng, Z. Hu, Y. Su, H. Li, M. Li, H. Guo, Y. Duan, W. Wang, M. Rao, J. Zheng, X. Wang, F. Pan, Optimized temperature effect of Li-ion diffusion with layer distance in Li(Ni<sub>x</sub>Mn<sub>y</sub>Co<sub>z</sub>)O<sub>2</sub> cathode materials for high performance Li-ion battery, *Adv. Energy Mater.* 6 (2016) 1–9.
- [115] A. Yaqub, Y.J. Lee, M.J. Hwang, S.A. Perviz, U. Farooq, J.H. Choi, D. Kim, H. Y. Choi, S.B. Cho, C.H. Doh, Low temperature performance of graphite and LiNi<sub>0.6</sub>Co<sub>0.2</sub>Mn<sub>0.2</sub>O<sub>2</sub> electrodes in Li-ion batteries, *J. Mater. Sci.* 49 (2014) 7707–7714.
- [116] P. Lyu, Y. Huo, Z. Qu, Z. Rao, Investigation on the thermal behavior of Ni-rich NMC lithium ion battery for energy storage, *Appl. Therm. Eng.* 166 (2020), 114749.
- [117] A. Aishova, G.T. Park, C.S. Yoon, Y.K. Sun, Cobalt-free high-capacity Ni-rich layered Li[Ni<sub>0.9</sub>Mn<sub>0.1</sub>]O<sub>2</sub> cathode, *Adv. Energy Mater.* 10 (2020), 1903179.
- [118] G. Li, Z. Huang, Z. Zuo, Z. Zhang, H. Zhou, Understanding the trace Ti surface doping on promoting the low temperature performance of LiNi<sub>1/3</sub>Co<sub>1/3</sub>Mn<sub>1/3</sub>O<sub>2</sub> cathode, *J. Power Sources* 281 (2015) 69–76.
- [119] B. Zhao, J. Xie, H. Zhuang, X. Liu, W. Li, X. Hu, Y. Jiang, J. Zhang, Improved low-temperature performance of surface modified lithium-rich Li<sub>1.2</sub>Ni<sub>0.13</sub>Co<sub>0.13</sub>Mn<sub>0.54</sub>O<sub>2</sub> cathode materials for lithium ion batteries, *Solid State Ionics* 347 (2020), 115245.
- [120] M.J. Lee, E. Lho, P. Bai, S. Chae, J. Li, J. Cho, Low-temperature carbon coating of nanosized Li<sub>1.015</sub>Al<sub>0.06</sub>Mn<sub>1.925</sub>O<sub>4</sub> and high-density electrode for high-power Li-ion batteries, *Nano Lett.* 17 (2017) 3744–3751.
- [121] J. Chen, S. Wang, D. Cai, H. Wang, Porous SiO<sub>2</sub> as a separator to improve the electrochemical performance of spinel LiMn<sub>2</sub>O<sub>4</sub> cathode, *J. Membr. Sci.* 449 (2013) 169–175.
- [122] G. Cai, R. Guo, L. Liu, Y. Yang, C. Zhang, C. Wu, W. Guo, H. Jiang, Enhanced low temperature electrochemical performances of LiFePO<sub>4</sub>/C by surface modification with Ti<sub>3</sub>SiC<sub>2</sub>, *J. Power Sources* 288 (2015) 136–144.
- [123] H.-H. Ryu, G.-C. Kang, R. Ismoyojati, G.-T. Park, F. Maglia, Y.-K. Sun, Intrinsic weaknesses of Co-free Ni–Mn layered cathodes for electric vehicles, *Mater. Today Off.* 56 (2022) 8–15.
- [124] P. Xiao, R. Luo, Z. Piao, C. Li, J. Wang, K. Yu, G. Zhou, H.-M.M. Cheng, High-performance lithium metal batteries with a wide operating temperature range in carbonate electrolyte by manipulating interfacial chemistry, *ACS Energy Lett.* 6 (2021) 3170–3179.
- [125] M. Ma, N.A. Chernova, B.H. Toby, P.Y. Zavalij, M.S. Whittingham, Structural and electrochemical behavior of LiMn<sub>0.4</sub>Ni<sub>0.4</sub>Co<sub>0.2</sub>O<sub>2</sub>, *J. Power Sources* 165 (2007) 517–534.
- [126] S. Jung, S. Park, T. Yoon, H. Kim, H. Jeong, J.H. Ryu, J.J. Kim, S.M. Oh, Low-temperature performance improvement of graphite electrode by allyl sulfide additive and its film-forming mechanism, *J. Electrochem. Soc.* 163 (2016) A1798–A1804.
- [127] D.J. Yoo, Q. Liu, O. Cohen, M. Kim, K.A. Persson, Z. Zhang, Understanding the role of SEI layer in low-temperature performance of lithium-ion batteries, *ACS Appl. Mater. Interfaces* 14 (2022) 11910–11918.
- [128] K. Kim, H. Ma, S. Park, N.S. Choi, Electrolyte-additive-driven interfacial engineering for high-capacity electrodes in lithium-ion batteries: promise and challenges, *ACS Energy Lett.* 5 (2020) 1537–1553.
- [129] E. Markevich, G. Salitra, D. Aurbach, Fluoroethylene carbonate as an important component for the formation of an effective solid electrolyte interphase on anodes and cathodes for advanced Li-ion batteries, *ACS Energy Lett.* 2 (2017) 1337–1345.
- [130] E. Markevich, G. Salitra, F. Chesneau, M. Schmidt, D. Aurbach, Very stable lithium metal stripping-plating at a high rate and high areal capacity in fluoroethylene carbonate-based organic electrolyte solution, *ACS Energy Lett.* 2 (2017) 1321–1326.
- [131] B. Liao, H. Li, M. Xu, L. Xing, Y. Liao, X. Ren, W. Fan, L. Yu, K. Xu, W. Li, Designing low impedance interface films simultaneously on anode and cathode for high energy batteries, *Adv. Energy Mater.* 8 (2018), 1800802.
- [132] W. Song, B. Hong, S. Hong, Y. Lai, J. Li, Y. Liu, Effect of prop-1-ene-1,3-sultone on the performances of lithium cobalt oxide/graphite battery operating over a wide temperature range, *Int. J. Electrochem. Sci.* 12 (2017) 10749–10762.
- [133] Y. Zhang, J. Luo, C. Wang, X. Hu, E. Matios, W. Li, Electrolyte additive enabled low temperature lithium metal batteries, *Mater. Chem. Front.* 6 (2022) 1405–1413.
- [134] M. Haruta, T. Okubo, Y. Masuo, S. Yoshida, A. Tomita, T. Takenaka, T. Doi, M. Inaba, Temperature effects on SEI formation and cyclability of Si nanoflake powder anode in the presence of SEI-forming additives, *Electrochim. Acta* 224 (2017) 186–193.
- [135] W. Zhao, J. Zheng, L. Zou, H. Jia, B. Liu, H. Wang, M.H. Engelhard, C. Wang, W. Xu, Y. Yang, J.G. Zhang, High voltage operation of Ni-rich NMC cathodes enabled by stable electrode/electrolyte interphases, *Adv. Energy Mater.* 8 (2018) 1–9.
- [136] H.M. Cho, M.V. Chen, A.C. MacRae, Y.S. Meng, Effect of surface modification on nano-structured LiNi<sub>0.5</sub>Mn<sub>1.5</sub>O<sub>4</sub> spinel materials, *ACS Appl. Mater. Interfaces* 7 (2015) 16231–16239.
- [137] Y. Dong, B.T. Young, Y. Zhang, T. Yoon, D.R. Heskett, Y. Hu, B.L. Lucht, Effect of lithium borate additives on cathode film formation in LiNi<sub>0.5</sub>Mn<sub>1.5</sub>O<sub>4</sub>/Li cells, *ACS Appl. Mater. Interfaces* 9 (2017) 20467–20475.
- [138] X. Fang, F. Lin, D. Nordlund, M. Mecklenburg, M. Ge, J. Rong, A. Zhang, C. Shen, Y. Liu, Y. Cao, M.M. Doeff, C. Zhou, Atomic insights into the enhanced surface stability in high voltage cathode materials by ultrathin coating, *Adv. Funct. Mater.* 27 (2017) 1–9.
- [139] Q. Zhang, R.E. White, Calendar life study of Li-ion pouch cells, *J. Power Sources* 173 (2007) 990–997.
- [140] S.-J. Yoon, S.-T. Myung, Y.-K. Sun, Low temperature electrochemical properties of Li[Ni<sub>x</sub>Co<sub>y</sub>Mn<sub>1-x-y</sub>]O<sub>2</sub> cathode materials for lithium-ion batteries, *J. Electrochem. Soc.* 161 (2014) A1514–A1520.
- [141] W. Lu, K. Xie, Z. Chen, S. Xiong, Y. Pan, C. Zheng, A new co-solvent for wide temperature lithium ion battery electrolytes: 2,2,2-Trifluoroethyl n-caproate, *J. Power Sources* 274 (2015) 676–684.
- [142] C. Zhu, W. Lv, J. Chen, C. Ou, Q. Zhang, H. Fu, H. Wang, L. Wu, S. Zhong, Butyl acrylate (BA) and ethylene carbonate (EC) electrolyte additives for low-temperature performance of lithium ion batteries, *J. Power Sources* 476 (2020), 228697.
- [143] J. Holoubek, M. Yu, S. Yu, M. Li, Z. Wu, D. Xia, P. Bhaladhare, M.S. Gonzalez, T. A. Pascal, P. Liu, Z. Chen, An all-fluorinated ester electrolyte for stable high-voltage Li metal batteries capable of ultra-low-temperature operation, *ACS Energy Lett.* 5 (2020) 1438–1447.
- [144] M.Z. Kufian, S.R. Majid, Performance of lithium-ion cells using 1 M LiPF<sub>6</sub> in EC/DEC (v/v = 1/2) electrolyte with ethyl propionate additive, *Ionics* 16 (2010) 409–416.
- [145] M.C. Smart, B.V. Ratnakumar, S. Surampudi, Use of organic esters as cosolvents in electrolytes for lithium-ion batteries with improved low temperature performance, *J. Electrochem. Soc.* 149 (2002) A361.
- [146] S. Herreyre, O. Huchet, S. Barusseau, F. Pertion, J.M. Bodet, P. Biensan, New Li-ion electrolytes for low temperature applications, *J. Power Sources* 97–98 (2001) 576–580.
- [147] M.C. Smart, B.V. Ratnakumar, K.B. Chin, L.D. Whitcanack, Lithium-ion electrolytes containing ester cosolvents for improved low temperature performance, *J. Electrochem. Soc.* 157 (2010), A1361.
- [148] B. Yang, H. Zhang, L. Yu, W.Z. Fan, D. Huang, Lithium difluorophosphate as an additive to improve the low temperature performance of LiNi<sub>0.5</sub>Co<sub>0.2</sub>Mn<sub>0.3</sub>O<sub>2</sub>/graphite cells, *Electrochim. Acta* 221 (2016) 107–114.
- [149] Q. Zhao, Y. Zhang, F. Tang, J. Zhao, S. Li, Mixed salts of lithium difluoro (oxalate) borate and lithium tetrafluoroborate electrolyte on low-temperature performance for lithium-ion batteries, *J. Electrochem. Soc.* 164 (2017) A1873–A1880.
- [150] W. Wang, T. Yang, S. Li, W. Fan, X. Zhao, C. Fan, L. Yu, S. Zhou, X. Zuo, R. Zeng, J. Nan, 1-ethyl-3-methylimidazolium tetrafluoroborate (EMI-BF<sub>4</sub>) as an ionic liquid-type electrolyte additive to enhance the low-temperature performance of LiNi<sub>0.5</sub>Co<sub>0.2</sub>Mn<sub>0.3</sub>O<sub>2</sub>/graphite batteries, *Electrochim. Acta* 317 (2019) 146–154.
- [151] T. Yang, W. Fan, C. Wang, Q. Lei, Z. Ma, L. Yu, X. Zuo, J. Nan, 2,3,4,5,6-Pentafluorophenyl methanesulfonate as a versatile electrolyte additive matches LiNi<sub>0.5</sub>Co<sub>0.2</sub>Mn<sub>0.3</sub>O<sub>2</sub>/graphite batteries working in a wide-temperature range, *ACS Appl. Mater. Interfaces* 10 (2018) 31735–31744.
- [152] A.S. Wotango, W.N. Su, A.M. Haregewoin, H.M. Chen, J.H. Cheng, M.H. Lin, C. H. Wang, B.J. Hwang, Designed synergetic effect of electrolyte additives to improve interfacial chemistry of MCMB electrode in propylene carbonate-based



- electrolyte for enhanced low and room temperature performance, *ACS Appl. Mater. Interfaces* 10 (2018) 25252–25262.
- [153] J. Kafil, J. Harris, J. Chang, J. Koshina, D. Boone, D. Qu, Development of wide temperature electrolyte for graphite/LiNiMnCoO<sub>2</sub> Li-ion cells: high throughput screening, *J. Power Sources* 392 (2018) 60–68.
- [154] L. Liao, P. Zuo, Y. Ma, Y. An, G. Yin, Y. Gao, Effects of fluoroethylene carbonate on low temperature performance of mesocarbon microbeads anode, *Electrochim. Acta* 74 (2012) 260–266.
- [155] L. Liao, T. Fang, X. Zhou, Y. Gao, X. Cheng, L. Zhang, G. Yin, Enhancement of low-temperature performance of LiFePO<sub>4</sub> electrode by butyl sulfone as electrolyte additive, *Solid State Ionics* 254 (2014) 27–31.
- [156] L. Liao, X. Cheng, Y. Ma, P. Zuo, W. Fang, G. Yin, Y. Gao, Fluoroethylene carbonate as electrolyte additive to improve low temperature performance of LiFePO<sub>4</sub> electrode, *Electrochim. Acta* 87 (2013) 466–472.
- [157] Q. Lei, T. Yang, X. Zhao, W. Fan, W. Wang, L. Yu, S. Guo, X. Zuo, R. Zeng, J. Nan, Lithium difluorophosphate as a multi-functional electrolyte additive for 4.4 V LiNi<sub>0.5</sub>Co<sub>0.2</sub>Mn<sub>0.3</sub>O<sub>2</sub>/graphite lithium ion batteries, *J. Electroanal. Chem.* 846 (2019).
- [158] K.M. Kim, N.V. Ly, J.H. Won, Y.G. Lee, W. Il Cho, J.M. Ko, R.B. Kaner, Improvement of lithium-ion battery performance at low temperature by adopting polydimethylsiloxane-based electrolyte additives, *Electrochim. Acta* 136 (2014) 182–188.
- [159] J. Shi, N. Ehteshami, J. Ma, H. Zhang, H. Liu, X. Zhang, J. Li, E. Paillard, Improving the graphite/electrolyte interface in lithium-ion battery for fast charging and low temperature operation: fluorosulfonyl isocyanate as electrolyte additive, *J. Power Sources* 429 (2019) 67–74.
- [160] I. Phiri, S. Ko, S. Kim, V.A. Afrifah, K. Lee, S.H. Kim, J.M. Ko, Zwitterionic osmolyte-inspired additives as scavengers and low temperature performance enhancers for lithium ion batteries, *Mater. Lett.* 288 (2021), 129366.
- [161] Y. Lin, X. Yue, H. Zhang, L. Yu, W. Fan, T. Xie, Using phenyl methanesulfonate as an electrolyte additive to improve performance of LiNi<sub>0.5</sub>Co<sub>0.2</sub>Mn<sub>0.3</sub>O<sub>2</sub>/graphite cells at low temperature, *Electrochim. Acta* 300 (2019) 202–207.
- [162] B. Liu, B. Li, S. Guan, Effect of fluoroethylene carbonate additive on low temperature performance of li-ion batteries, *Electrochem. Solid State Lett.* 15 (2012) 2012–2014.
- [163] S.S. Zhang, K. Xu, T.R. Jow, A new approach toward improved low temperature performance of Li-ion battery, *Electrochem. Commun.* 4 (2002) 928–932.
- [164] Z. Zhang, T. Hu, Q. Sun, Y. Chen, Q. Yang, Y. Li, The optimized LiBF<sub>4</sub> based electrolytes for TiO<sub>2</sub>(B) anode in lithium ion batteries with an excellent low temperature performance, *J. Power Sources* 453 (2020), 227908.
- [165] G. Xu, S. Huang, Z. Cui, X. Du, X. Wang, D. Lu, X. Shangguan, J. Ma, P. Han, X. Zhou, G. Cui, Functional additives assisted ester-carbonate electrolyte enables wide temperature operation of a high-voltage (5 V-Class) Li-ion battery, *J. Power Sources* 416 (2019) 29–36.
- [166] H. Chen, B. Liu, Y. Wang, H. Guan, H. Zhou, Insight into wide temperature electrolyte based on lithiumdifluoro(oxalate)borate for high voltage lithium-ion batteries, *J. Alloys Compd.* 876 (2021), 159966.
- [167] S. Tan, U.N.D. Rodrigo, Z. Shadik, B. Lucht, K. Xu, C. Wang, X.-Q. Yang, E. Hu, Novel low-temperature electrolyte using isoxazole as the main solvent for lithium-ion batteries, *ACS Appl. Mater. Interfaces* 13 (2021) 24995–25001.
- [168] L. Hamenu, H.S. Lee, M. Latifatu, K.M. Kim, J. Park, Y.G. Baek, J.M. Ko, R. B. Kaner, Lithium-silica nanosalt as a low-temperature electrolyte additive for lithium-ion batteries, *Curr. Appl. Phys.* 16 (2016) 611–617.
- [169] Q. Li, S. Jiao, L. Luo, M.S. Ding, J. Zheng, S.S. Cartmell, C.M. Wang, K. Xu, J. G. Zhang, W. Xu, Wide-temperature electrolytes for lithium-ion batteries, *ACS Appl. Mater. Interfaces* 9 (2017) 18826–18835.
- [170] X. Fan, X. Ji, L. Chen, J. Chen, T. Deng, F. Han, J. Yue, N. Piao, R. Wang, X. Zhou, X. Xiao, L. Chen, C. Wang, All-temperature batteries enabled by fluorinated electrolytes with non-polar solvents, *Nat. Energy* 4 (2019) 882–890.
- [171] J. Xu, X.X. Wang, N. Yuan, J. Ding, S. Qin, J.M. Razal, X.X. Wang, S. Ge, Y. Gogotsi, Extending the low temperature operational limit of Li-ion battery to –80 °C, *Energy Storage Mater.* 23 (2019) 383–389.
- [172] X.X. Zhang, Z.F. Wang, C.H. Li, J.H. Liu, Q.L. Zhang, FEC-LiTFSI-Pyr1ATFSI ionic liquid electrolyte to improve low temperature performance of lithium-ion batteries, *Adv. Mater. Res.* 986–987 (2014) 80–83.
- [173] W. Lv, C. Zhu, J. Chen, C. Ou, Q. Zhang, S. Zhong, High performance of low-temperature electrolyte for lithium-ion batteries using mixed additives, *Chem. Eng. J.* 418 (2021), 129400.
- [174] S. Kuang, H. Hua, P. Lai, J. Li, X. Deng, Y. Yang, J. Zhao, Anion-containing solvation structure reconfiguration enables wide-temperature electrolyte for high-energy-density lithium-metal batteries, *ACS Appl. Mater. Interfaces* 14 (2022) 19056–19066.
- [175] M.C. Smart, B.V. Ratnakumar, L.D. Whitcanack, Performance of low temperature electrolytes in experimental and prototype Li-ion cells, *Collect. Tech. Pap. - 5th Int. Energy Convers. Eng. Conf.* 1 (2007) 395–405.
- [176] A.J. Ringsby, K.D. Fong, J. Self, H.K. Bergstrom, B.D. McCloskey, K.A. Persson, Transport phenomena in low temperature lithium-ion battery electrolytes, *J. Electrochem. Soc.* 168 (2021), 080501.
- [177] S.S. Zhang, K. Xu, J.L. Allen, T.R. Jow, Effect of propylene carbonate on the low temperature performance of Li-ion cells, *J. Power Sources* 110 (2002) 216–221.
- [178] M. Kasprzyk, A. Zalewska, L. Niedzicki, A. Bitner, M. Marcinek, W. Wiecek, Non-crystallizing solvent mixtures and lithium electrolytes for low temperatures, *Solid State Ionics* 308 (2017) 22–26.
- [179] H. Fan, X. Liu, L. Luo, F. Zhong, Y. Cao, All-Climate high-voltage commercial lithium-ion batteries based on propylene carbonate electrolytes, *ACS Appl. Mater. Interfaces* 14 (2022) 574–580.
- [180] S.V. Sazhin, M.Y. Khimchenko, Y.N. Tritenichenko, H.S. Lim, Performance of Li-ion cells with new electrolytes conceived for low-temperature applications, *J. Power Sources* 87 (2000) 112–117.
- [181] J. Li, C.F. Yuan, Z.H. Guo, Z.A. Zhang, Y.Q. Lai, J. Liu, Limiting factors for low-temperature performance of electrolytes in LiFePO<sub>4</sub>/Li and graphite/Li half cells, *Electrochim. Acta* 59 (2012) 69–74.
- [182] Q. Li, D. Lu, J. Zheng, S. Jiao, L. Luo, C.M. Wang, K. Xu, J.G. Zhang, W. Xu, Li<sup>+</sup>-Desolvation dictating lithium-ion battery's low-temperature performances, *ACS Appl. Mater. Interfaces* 9 (2017) 42761–42768.
- [183] S. Lei, Z. Zeng, M. Liu, H. Zhang, S. Cheng, J. Xie, Balanced solvation/de-solvation of electrolyte facilitates Li-ion intercalation for fast charging and low-temperature Li-ion batteries, *Nano Energy* 98 (2022), 107265.
- [184] S.S. Zhang, K. Xu, T.R. Jow, Electrochemical impedance study on the low temperature of Li-ion batteries, *Electrochim. Acta* 49 (2004) 1057–1061.
- [185] L. Yu, S. Chen, H. Lee, L. Zhang, M.H. Engelhard, Q. Li, S. Jiao, J. Liu, W. Xu, J. G. Zhang, A localized high-concentration electrolyte with optimized solvents and lithium difluoro(oxalate)borate additive for stable lithium metal batteries, *ACS Energy Lett.* 3 (2018) 2059–2067.
- [186] J. Holoubek, K. Kim, Y. Yin, Z. Wu, H. Liu, M. Li, A. Chen, H. Gao, G. Cai, T. A. Pascal, P. Liu, Z. Chen, Electrolyte design implications of ion-pairing in low-temperature Li metal batteries, *Energy Environ. Sci.* 15 (2022) 1647–1658.
- [187] Z. Piao, P. Xiao, R. Luo, J. Ma, R. Gao, C. Li, J. Tan, K. Yu, G. Zhou, H.M. Cheng, Constructing a stable interface layer by tailoring solvation chemistry in carbonate electrolytes for high-performance lithium-metal batteries, *Adv. Mater.* 34 (2022), 2108400.
- [188] B.K. Mandal, A.K. Padhi, Z. Shi, S. Chakraborty, R. Filler, New low temperature electrolytes with thermal runaway inhibition for lithium-ion rechargeable batteries, *J. Power Sources* 162 (2006) 690–695.
- [189] J. Yuan, N. Qin, Y. Lu, L. Jin, J. Zheng, J.P. Zheng, The effect of electrolyte additives on the rate performance of hard carbon anode at low temperature for lithium-ion capacitor, *Chin. Chem. Lett.* 33 (2022) 3889–3893.
- [190] M.C. Smart, B.L. Lucht, S. Dalavi, F.C. Krause, B.V. Ratnakumar, The effect of additives upon the performance of MCMB/LiNi<sub>x</sub>Co<sub>1-x</sub>O<sub>2</sub> Li-ion cells containing methyl butyrate-based wide operating temperature range electrolytes, *J. Electrochem. Soc.* 159 (2012) A739–A751.
- [191] J.-P. Jones, M.C. Smart, F.C. Krause, R.V. Bugga, The effect of electrolyte additives upon lithium plating during low temperature charging of graphite-LiNiCoAlO<sub>2</sub> lithium-ion three electrode cells, *J. Electrochem. Soc.* 167 (2020), 020536.